

11-5-2021

## Development of a Miniature Pipe Crawler for Application in Fossil Energy Power Plants

Caique C. Lara

Florida International University, clara021@fiu.edu

Follow this and additional works at: <https://digitalcommons.fiu.edu/etd>



Part of the [Other Mechanical Engineering Commons](#)

---

### Recommended Citation

Lara, Caique C., "Development of a Miniature Pipe Crawler for Application in Fossil Energy Power Plants" (2021). *FIU Electronic Theses and Dissertations*. 4853.

<https://digitalcommons.fiu.edu/etd/4853>

This work is brought to you for free and open access by the University Graduate School at FIU Digital Commons. It has been accepted for inclusion in FIU Electronic Theses and Dissertations by an authorized administrator of FIU Digital Commons. For more information, please contact [dcc@fiu.edu](mailto:dcc@fiu.edu).

FLORIDA INTERNATIONAL UNIVERSITY

Miami, Florida

DEVELOPMENT OF A MINIATURE PIPE CRAWLER FOR APPLICATION IN  
FOSSIL ENERGY POWER PLANTS

A thesis submitted in partial fulfillment of

the requirements for the degree of

MASTER OF SCIENCE

in

MECHANICAL ENGINEERING

by

Caique Costa Lara

2021

To: Dean L. Volakis  
College of Engineering and Computing

This thesis, written by Caique Costa Lara, and entitled Development of a Miniature Pipe Crawler for Application in Fossil Energy Power Plants, having been approved in respect to style and intellectual content, is referred to you for judgment.

We have read this thesis and recommend that it be approved.

---

Aparna Aravelli

---

Benjamin Boesl

---

Dwayne McDaniel, Major Professor

Date of Defense: November 5, 2021

The thesis of Caique Costa Lara is approved.

---

Dean John Volakis  
College of Engineering and Computing

---

Andres G. Gil  
Vice President for Research and Economic Development  
and Dean of the University Graduate School

Florida International University, 2021

## DEDICATION

“O céu é para você,  
o que você traz no coração  
para dar aos outros”

–Fernando Antônio Lara

## ACKNOWLEDGMENTS

Firstly, I would like to acknowledge the support of my advisor, Professor Dwayne McDaniel. His mentorship throughout the project and subsequent thesis made the late nights and long hours worthwhile. It has been my privilege to have had the opportunity to work under his guidance for the past two years.

As well, a huge thank you to the people who helped develop the project; Dr. Aparna Aravelli and Dr. Benjamin Boesl - for their valuable counseling and support, Mr. Anthony Abrahao - for his friendship and patience while teaching me robotics, and Julie Villamil - for her lab comradery and dedication to this work. Her advice allowed me to learn from her past mistakes, saving hours of work.

My deepest thanks to Kelsey Boyd for your support, kindness, and love. It would have been so hard without you. A big thanks to Guilherme Daldegan, who made everything possible; I wouldn't be here without you, thank you for your support and friendship over the past years.

I would like to thank the Applied Research Center and the Mechanical and Materials Engineering Department at Florida International University for the opportunity and experience. I am incredibly grateful for the care that went into providing the excellent personnel and facilities furthering student development.

Last but not least, I would like to acknowledge DOE-NETL for their financial support, which was funded under Award Number DE-FE0031651.

Thank you.

ABSTRACT OF THE THESIS  
DEVELOPMENT OF A MINIATURE PIPE CRAWLER FOR APPLICATION IN  
FOSSIL ENERGY POWER PLANTS

by

Caique Costa Lara

Florida International University, 2021

Miami, Florida

Professor Dwayne McDaniel, Major Professor

The power generation of fossil fuel power plants relies on burning coal to generate steam. The heat exchange between the water and burned coal occurs in the combustion chamber, which operates at a high pressure and temperature. Monitoring the integrity of the tubes inside the combustion chamber is a key factor to avoid failures. However, this is not an easy task as some areas are hard to reach and the tubes typically have a complex geometry. Moreover, the inspections are usually manual, external and the environment is hazardous for humans. This thesis presents the development and testing of an electrically powered pipe crawler that can navigate inside 5 cm diameter tubes and provide an assessment of their health. The crawler utilizes peristaltic motion within the tubes via interconnected modules for gripping and extending. The modular nature of the system allows it to traverse through straight sections and multiple 90° and 180° bends. Additional modules in the system include an ultrasonic sensor for tube thickness measurements, as well as environmental sensors, a LiDAR and a camera. These modules utilize a gear system that allows for 360° rotation and provide a means of inspecting the entire internal circumference of the tubes. Bench and engineering scale testing proved the robot's ability to navigate and perform inspections inside 50.8 mm diameter pipes.

## TABLE OF CONTENTS

CHAPTER	PAGE
1 INTRODUCTION	1
1.1 MOTIVATION . . . . .	1
1.2 SCOPE . . . . .	2
1.3 CHALLENGES . . . . .	3
1.4 APPROACH . . . . .	4
1.5 CONTRIBUTIONS . . . . .	6
2 LITERATURE REVIEW	8
2.1 FOSSIL FUEL POWER PLANTS . . . . .	8
2.2 NON-DESTRUCTIVE TECHNIQUES . . . . .	12
2.3 INSPECTION ROBOTS . . . . .	15
2.3.1 EXTERNAL INSPECTION ROBOTS . . . . .	16
2.3.2 INTERNAL INSPECTION ROBOTS . . . . .	19
3 SYSTEM DESCRIPTION	23
3.1 GENERAL SPECIFICATIONS . . . . .	23
3.1.1 LOCOMOTION SYSTEM . . . . .	24
3.1.2 KINEMATIC ANALYSIS . . . . .	25
3.1.3 ACTUATORS . . . . .	27
3.2 PERISTALTIC MODULES . . . . .	28
3.2.1 GRIPPER MODULE . . . . .	30
3.2.2 EXTENDER MODULE . . . . .	31
3.2.3 ELECTRONICS MODULE . . . . .	33
3.3 INSPECTION MODULES . . . . .	34
3.3.1 INSTRUMENTATION MODULE . . . . .	34
3.3.2 UT SENSOR MODULE . . . . .	37
3.3.3 SURFACE PREPARATION MODULE . . . . .	39
3.4 SYSTEM INTEGRATION . . . . .	41
3.4.1 STABILIZATION MECHANISM . . . . .	41
3.4.2 COMMUNICATION SYSTEM . . . . .	42
4 TESTING	44
4.1 BENCH SCALE TESTING . . . . .	44
4.1.1 PERISTALTIC CRAWLER . . . . .	44
4.1.2 INSTRUMENTATION MODULE . . . . .	46
4.1.3 ULTRASONIC TRANSDUCER MODULE . . . . .	47
4.1.4 SURFACE PREPARATION MODULE . . . . .	49
4.2 ENGINEERING SCALE TESTING . . . . .	49
5 CONCLUSION AND RECOMMENDATIONS	53
5.1 RECOMMENDATIONS . . . . .	53
5.1.1 MECHANICAL DESIGN . . . . .	53
5.1.2 ELECTRONICS . . . . .	54
5.1.3 COMMUNICATION PROTOCOL . . . . .	55

5.2 CONCLUSION AND FUTURE WORK . . . . .	55
BIBLIOGRAPHY	57

## LIST OF FIGURES

FIGURE	PAGE
1.1 Failed section of a superheater tube. . . . .	1
1.2 Superheater tubes inspection. . . . .	3
1.3 Conceptual design of the proposed inspection system. . . . .	5
2.1 Heat recover steam generator with forced circulation system. . . . .	10
2.2 Super heater header and tubes. . . . .	10
2.3 Examples of permanent deformation of tubes. . . . .	11
2.4 Point cloud model of a pipe created using LiDAR. . . . .	13
2.5 Technology comparison between UT and EMAT sensors. . . . .	14
2.6 Robotic platform with magnetic caterpillar traction system. . . . .	16
2.7 Robotic platform with propeller system. . . . .	17
2.8 HydroFORM inspection tool. . . . .	18
2.9 Mechanical architecture of internal inspection robots. . . . .	19
2.10 Wheeled type robot. . . . .	20
2.11 Caterpillar type robot. . . . .	21
2.12 Inchworm type robot. . . . .	22
3.1 Schematic of the pipe elbows. . . . .	23
3.2 Peristaltic locomotion of the robotic crawler. . . . .	25
3.3 Parameters to determine the module's size. . . . .	25
3.4 Diagram illustrating changes on the length and width for the robotic modules. . . . .	26
3.5 180° bend kinematics. . . . .	27
3.6 Electric motors. . . . .	28
3.7 Peristaltic motion of the crawler. . . . .	29
3.8 Gripper module. . . . .	30
3.9 Assembled gripper module. . . . .	31
3.10 Schematic of the extender module. . . . .	32
3.11 Assembled extender module. . . . .	33
3.12 Electronics module. . . . .	34
3.13 Schematic of the instrumentation module. . . . .	35
3.14 Instrumentation module assembled. . . . .	36
3.15 Slip-ring. . . . .	37
3.16 Schematic of the ultrasonic transducer module. . . . .	38
3.17 UT sensor module and PCB. . . . .	39
3.18 Schematic of the surface preparation module. . . . .	40
3.19 Surface preparation module. . . . .	41
3.20 Stabilization mechanism. . . . .	42
3.21 CAN Bus architecture. . . . .	42
3.22 Tether configuration for the crawler system. . . . .	43
4.1 Robotic crawler traveling in straight tube section. . . . .	45
4.2 Robotic crawler traveling in a plastic 180° bend. . . . .	45
4.3 Instrumentation module testing. . . . .	46

4.4	Slip ring testing. . . . .	47
4.5	Measurements performed on the tube's inner surface. . . . .	47
4.6	Thickness measurements obtained from the inside and outside surfaces of a tube with varying thicknesses. . . . .	48
4.7	Surface preparation module. . . . .	49
4.8	Engineering scale test mockup. . . . .	50
4.9	Tether load averaged. . . . .	51
4.10	Crawler navigating the superheater tube mock-up with magnified images. . . . .	51
5.1	Integrated crawler system (inspection tool) concept. . . . .	56

# 1. INTRODUCTION

## 1.1 MOTIVATION

Routine inspection and preventive maintenance are fundamental factors that help to avoid failures and significant accidents. The last two decades have seen a considerable increase in the maintenance and inspection fields, which is due to industries' constant pursuance of profit, quality, and safety [24].

Industrial equipment needs a periodic inspection to verify the integrity of its components. During the inspection, it can be determined if any maintenance is required. The mechanical systems of fossil fuel powerplants are no different. Commonly, a superheater power plant operates by heating water to generate steam and produce energy. This process has several mechanical components that can fail if maintenance is not executed on time.

The combustion chamber, for example, operates in temperatures as high as 540°C and pressures that can reach 1000 bar [13]. These conditions are aggressive for the superheater tubes, which promote heat exchange within the water and hot flue gases. Therefore, a prolonged operation of those components with a lack of maintenance can cause surface oxidation and plastic deformation [2]. If these defects are not detected and repaired, they can cause a rupture of the tubes (Figure 1.1). Failure of the high-pressure tubes is dangerous and might cause the plant's closure for repair.



Figure 1.1: Failed section of a superheater tube [2].

Periodic inspections must be conducted to avoid catastrophic failures in superheater tubes. Typically, this process is manual, laborious, and time-consuming. Moreover, these components are typically installed in hazardous and hard-to-reach areas. Innovation in inspection technologies has consequently seen an increase in demand. In addition, efforts to improve operational efficiency and increase the reliability of inspections has led to new outcomes in this subject.

More recent technologies utilize robots as an alternative to human-based inspection. These systems overcome challenges faced by traditional methods while keeping the inspector away from the unsafe environment of the combustion chamber. By developing an inspection tool that can monitor the integrity of superheater tubes, a solution is created for today's industry demands.

## 1.2 SCOPE

Inspection methods of superheater tubes, either from outside or inside, commonly utilize non-destructive techniques (NDT) to assess the integrity of the pipes. Furthermore, different restrictions can limit the inspection capabilities.

When access is permissible, inspection from the outside is the easiest way to verify the tube's integrity. On external inspections, sensors such as ultrasonic transducer (UT) or electromagnetic acoustic transducer (EMAT) are commonly used. In addition, visual inspection using a camera can further assist in the evaluation.

To assess the integrity of pipes from inside, a borescope is commonly utilized. The equipment consists of a flexible tube with a camera on the tip, providing visual inspection. Although simple, the technique is limited by the bends of the pipeline and does not allow for long pipe length inspection.

Manual inspections are known to be laborious and time-consuming. An inspector must enter inside the combustion chamber and perform the inspection of the tubes, as shown in Figure 1.2. Therefore, personal protective equipment and confined space certification courses are often required. Additionally, the environment inside the combustion

chamber is hazardous for humans as the environment is dirty and oxygen levels may be low.



Figure 1.2: Superheater tubes inspection.

The plant also needs to shut down to perform the inspection, leading to financial implications. Moreover, the pipes have limited space between them, making it impossible to reach some areas for inspection. These situations cause the manual inspection to be costly and ineffective for non-accessible areas of the tubes.

This research aims to address the challenges related to the inspection of superheater powerplants. As a result, an internal inspection robot that can navigate through several  $90^\circ$  and  $180^\circ$  bends and provide data to validate the integrity of the pipes was designed and manufactured. In addition, the robot utilizes electronic sensors and a UT sensor for wall thickness measurement.

### 1.3 CHALLENGES

In-pipe inspection tools face several constraints that limit the robot's capabilities. The space is limited and the pipeline has several  $180^\circ$  bends. In addition, degradation of the pipeline can obstruct the sensors and complicate the inspection process.

In the field of inspection robotics, the task of evaluating the integrity of pipelines poses several challenges. One of the primary factors to be considered is the generation of traction within the environment. Robotic platforms that navigate on tubes commonly

have complex designs and several factors can lead to failures. Furthermore, most off-the-shelf products are not designed for that purpose, and some adaptation may be required.

The coiled structure of superheater tubes poses another challenge. For example, a typical pipeline of a fossil energy powerplant contains several 90° and 180° bends. When the robot navigates through multiple bends, the tether load increases significantly. Therefore, the inspection platform needs to be flexible and have adequate pull force capability to address the issues regarding the pipeline structure.

Besides the complex structure of the pipeline it is expected a level of degradation on the tubes such as erosion, scaling, and thermal expansion. Moreover, the interior of the pipeline can be irregular and contain rust or material deposition. The robotic platform needs to navigate through this environment and detect the areas that need maintenance. In addition, some sensors cannot take measurements within dirty surfaces, potentially requiring a prior cleaning.

Another critical feature required of the robotic platform is the capability of collecting valuable data to assay the integrity of the pipeline. Unfortunately, commercial products do not offer the requirements needed. For example, small electronics do not have a good resolution and do not function well for small ranges. In addition, ultrasonic transducer probes are sizable to embed and their measurements can fluctuate in curved surfaces.

Developing a robotic platform to overcome the challenges mentioned above is not an easy task. Meeting the requirements heavily depends on proper decisions for the physical design, actuators, and controllers. The compromise between maneuverability and design simplicity is an essential consideration for the project.

#### 1.4 APPROACH

This research aims to design a robotic platform to inspect superheater tubes with minimal human intervention. The system provides information regarding the structural integrity of crucial pipeline components in fossil fuel power plants that are not easily accessible.

The system consists of a tethered pipe crawler that can navigate through pipes commonly found in superheater powerplants. A robust operation for the robotic platform requires that the system can navigate in this environment. Multiple units might be needed for the proposed crawler system, depending on the distance traveled. As shown in Figure 1.3, the use of auxiliary crawlers will assist in distributing the tether load and extend the length of pipes inspected.

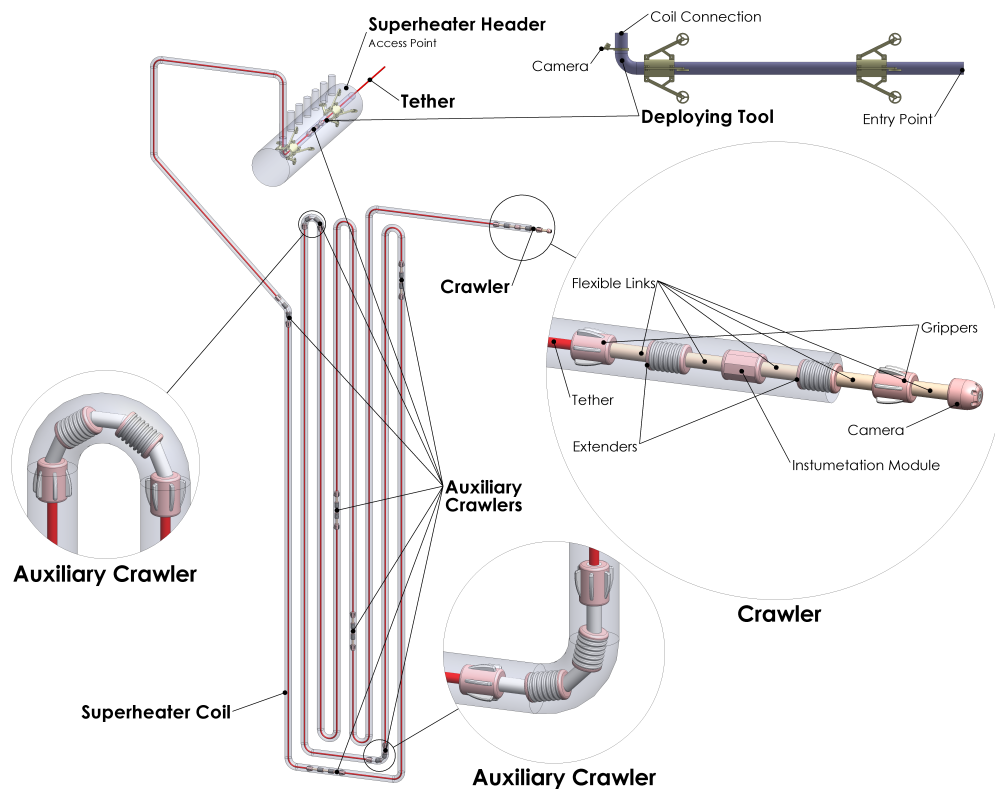


Figure 1.3: Conceptual design of the proposed inspection system.

The initial crawler system houses sensors that can be used to determine the health of pipes. The sensor module includes an optical camera, light detection and ranging (LiDAR) sensor, and an ultrasonic transducer sensor, which can be used to obtain thickness measurements of the pipes. To be able to perform the inspection, the superheater tubes will need to be out of operation and not flooded. Limiting the robotic platform to this application simplifies the design, as the robot will not face high temperatures and a waterproof platform will not be required.

The robot is modular and consists of several segments, which are 3-D printed and use off-the-shelf components. Some machined and metal parts are also included to increase the mechanical efficiency and improve the robot's reliability. Bench-scale testing was conducted to ensure that the proposed design can navigate through long pipe distances. The superheater tubes environment is simulated in a mockup, containing several 180° bends and straight sections to prove the system's capability to navigate the coiled structure. Moreover, tests were conducted to determine how the tether load varies as the pipe length increases and as the robot navigates through more bends. These tests provide a better understanding of the specific force load requirements.

## 1.5 CONTRIBUTIONS

This research effort aims to contribute to two main topics for in-pipe robotic systems. The first is the development of a peristaltic crawler for small diameter pipe systems. The second contribution is to create inspection modules that provide information regarding key pipeline components' structural integrity, which can be utilized in fossil fuel power plants.

Robots offer a number of benefits over human inspection. The advantages of using such a system include removing a human from hazardous environments, the reduced time spent on inspections, and data reliability. The robotic inspection tool developed in this effort, also improves the state-of-the-art as a novel application for superheater tubes and coiled structures. However, drawbacks include the necessity of the plant to be shut down, which can be costly.

A significant contribution of this research is developing a peristaltic robot capable of navigating through 50.8 millimeters tubes containing several 90° and 180° bends. Furthermore, the robotic platform is capable of navigate through long pipeline distances and manufactured with commercially available components and 3-D printed parts. With custom design components the robotic platform could potentially navigate through longer pipe distances.

Another contribution of this research is to provide information regarding the integrity of general piping systems. An example within the fossil fuel power plants is the superheater coils. With slight modifications to the crawler's design, it could be easily applicable for other pipe systems with similar diameters. The robotic platform includes multiple crawlers tethered together, with the initial system containing the sensors and verifying the the tube integrity.

- Caique Lara et al. "Development of an Innovative Inspection Tool for Super heater Tubes in Fossil Fuel Power Plants". In: *Materials Evaluation* 79.7 (July 2021), pp. 728–738. DOI:10.32548/2021.ME-04212.

## 2. LITERATURE REVIEW

The inspection of pipelines using robotic systems has increased in recent years. This research seeks to improve the state-of-the-art as it utilizes NDT methods for integrity analysis and is designed to operate in small pipe diameters.

This chapter introduces an overview of the systems and subsystems of superheater powerplants. The pipeline inside the combustion chamber is analyzed and a better understanding of its coiled structure is provided. A further examination of some of the most common defects of superheater tubes is presented and assists in understanding how these deformities propagate and what can be done to detect them.

The following section introduces the most common non-destructive techniques utilized to inspect pipelines. An overview of the requirements and restrictions for some NDTs supports the decision-making for the sensors used in the robotic platform presented in this research. Knowing the defects that a pipeline may have and the techniques utilized to detect them is a starting point for developing the robotic platform.

In addition, a review of automated tools for pipeline inspection and their capabilities is presented. Some of the work is introduced by academia and others are already utilized in the industry. These mechanisms support the development of this research, as they present restrictions and functionalities for each project.

### 2.1 FOSSIL FUEL POWER PLANTS

Fossil fuel has been used as a source for power generation since ancient times [28]. However, it was during the eighteenth century that its use grew exponentially. The rise of electric applications served as a factor to widespread the use of burning fossil fuels to produce steam and generate power [28]. This fuel is used as the main source of power generation in the United States and represents about 60% of all the electricity generated in the country [46].

Burning fossil fuel to produce heat is the most common way to utilize it. Boiler systems are used to extract the thermal energy of the fuel and convert it to electric energy. The heating system contains tubes to promote the heat exchange between the water and the burned fuel. This process is utilized in fossil fuel powerplants, which use superheated steam to produce electricity [40]. From the total energy produced in the United States, natural gas represents 40.3%, while coal 19.3%. Petroleum and other gases represent the remaining 0.7% [46].

Two main types of boilers are used in the industry: fire and water tube boilers. The flue gases pass inside the tubes in the fire tube boilers, while the water runs outside in a sealed container. The heat transfer occurs through the wall of the tubes by thermal conduction. Due to its design, fouling of ash may occur in the interior of tubes, causing erosion. Fire tube boilers are utilized for small steam requirements in the industry and are limited by the size and pressure-holding capacities of the shell. These systems commonly have low thermal efficiency due to its design [40]. This type of boiler is unsuitable for large power generation plants and will not be focused on in this research.

Water-tube boilers exchange heat between the fuel and the superheated steam in the combustion chamber. The heat recovery steam generator consists of several subsystems in the flow gas stream. First, water is inserted into the economizer to pre-heat and will vaporize in the evaporator. Next, the saturated steam increases its temperature and pressure while passing through the pipes of the superheater, turning into superheated steam. Finally, the superheated steam is passed through the turbines, which will transform the thermal energy of the steam to mechanical energy and subsequently into electrical energy [28]. Figure 2.1 represents a primary circuit for steam generators.

The system uses several tubes to increase the heat exchange between the water and gas flow. The pipes can be made of different materials and may have varying sizes between superheater sections. The material of the pipelines is characterized as high-quality steel with low carbon, and the tubes are produced and tested under specific standards.

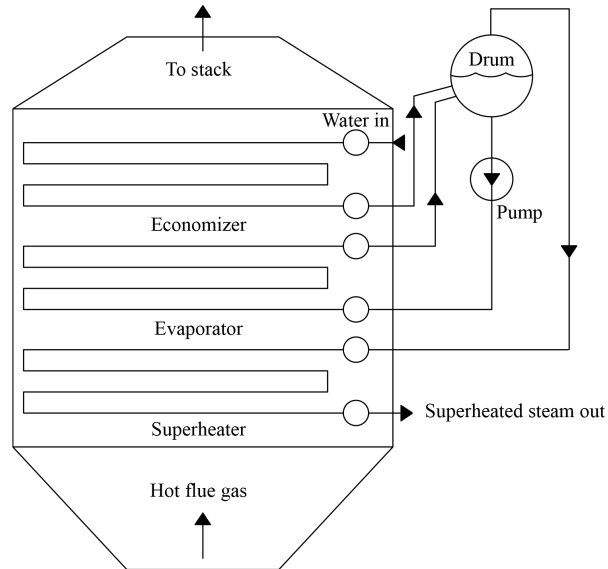


Figure 2.1: Heat recover steam generator with forced circulation system.

They range from 1.3 to 7.6 cm in diameter and operate at temperatures up to 540°C and pressures between 10 to 1000 bar [13].

The multipass cross-flow exchangers are the most common type for the superheater tubes [43]. This type of boiler utilizes several tubes in a coiled structure with several 90° and 180° bends. The pipes are connected using top and bottom headers, which distribute the water within the pipes. The system is designed to extract the maximum amount of heat from the flue gas. Figure 2.2 shows an example of a superheater header and its tube section.



Figure 2.2: Super heater header and tubes [22].

The heat distribution on the tubes is a crucial factor for the non-propagation of failures. The heat exchange throughout the tube surface must be uniform, as small temperature variations can lead to failure. If the heat is exchanged unevenly, small cracks can occur, leading to the tubes' collapse [21]. Moreover, the elevated temperature in the tubes generates the potential for increased levels of corrosion and erosion.

Additionally, there can be external deposits of slag and ash fouling on the tubes. Material deposition inside the tubes can occur if there are any contaminants in the water. These types of material deposition can lead to failures due to uneven heat exchange in the area. Figure 2.3 shows some of the most common failures that can occur within the pipes inside the combustion chamber of fossil fuel powerplants.

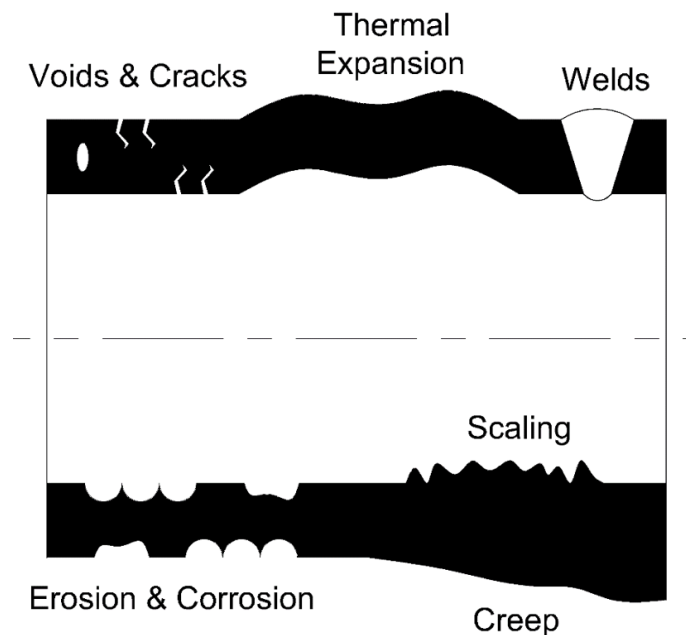


Figure 2.3: Examples of permanent deformation of tubes.

New technologies and manufacturing processes allow superheater tubes to operate at higher pressures and temperatures, increasing the plant efficiency. However, the environment is more aggressive, and failures in the system can lead to increased downtime for the plant, reduced power, and a high cost for repairs. Detection of this type of degradation is possible using standard NDTs. Some of the most common inspection practices are presented in the next section.

## 2.2 NON-DESTRUCTIVE TECHNIQUES

Non-destructive techniques has been an area of continuous growth for over sixty years [9]. The technique is commonly used in various engineering fields like aerospace, metallurgical engineering, and material science. Moreover, NDTs are very popular in the industry due to their flexibility and relative cost-effectiveness. It is mainly used for the routine inspection of industrial processes and structures. However, with the industries' willingness to improve their products' reliability and quality, NDTs have gained more importance in recent years [38].

Among the most common NDTs, visual inspection is largely utilized [7]. This approach allows for surface inspection with the use of a camera. The method is effective in detecting large cracks and superficial corrosion. Although, visual inspection is limited in the detection of minor defects [10]. Better detection of deformities may require cleaning or coat removal. In addition, some areas can be hard to reach or have limited space, reducing the performance of the inspection. However, the use of equipment such as a borescope can enhance the evaluation of the mentioned areas.

Other optical methods includes LiDAR sensors, which use a laser to identify and measure the distance of a target [33]. LiDAR sensors works by emitting a pulse of laser light on an object; the sensor's receiver then measures the amount of reflected light and the time taken to return the pulse, also known as the time of flight. The time spent on the process is converted by the sensor into distance. This technique is effective for detecting some abnormalities on the surface and works well on matte surfaces. However, highly reflective or absorbent materials deflect or completely absorb the beam, leading to inaccurate measurements [44]. The sensor can be swept several times across the environment to create a two-dimensional point cloud. For 3-D mapping, the LiDAR can be translated on an additional axis. Figure 2.4 shows an example of point cloud model of a wastewater pipe created using LiDAR sensor.

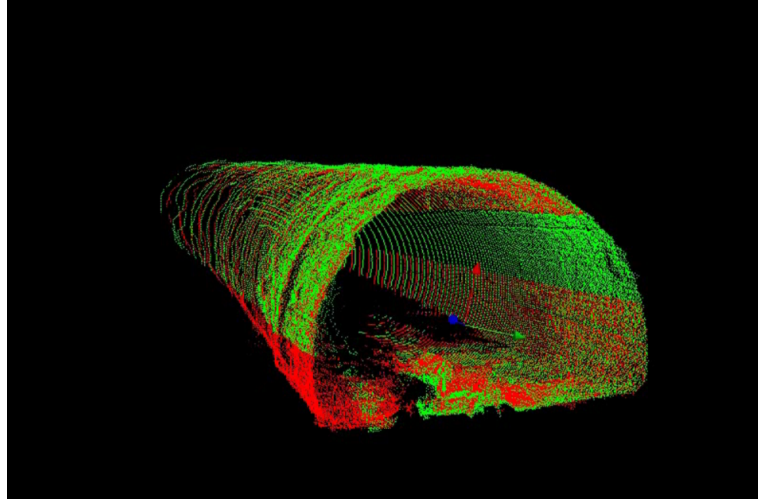


Figure 2.4: Point cloud model of a pipe created using LiDAR [3].

To further evaluate the degradation of walls, UT sensors can be used. The UT gauge transmits sound waves to the surface of the equipment through a probe. The sensor calculates the thickness of metallic or non-metallic surfaces by measuring the time of flight of the sound wave. The wavelength transmitted can be adjusted to measure wall or coating thickness [37]. Two types of sound waves can be used, transverse and longitudinal. They govern the direction that the sound wave travels in the material and can affect the detectable size of imperfections on the surface being inspected [31].

Measurements of wall thickness using UT probe require the inspected area to be clean to obtain accurate results. Moreover, the sensor typically requires a fluid couplant between the probe and the wall. The couplant removes the air gap and allows the sound wave to travel from the probe to the equipment and then back to the probe. Examples of couplant that can be utilized include couplant gel, grease, or water. The optimal utilization for the sensor is on flat surfaces. When measuring the wall thicknesses of curved surfaces, a curved surface correction (CSC) may be applied [1]. This phenomenon occurs due to the refraction of the sound wave in the material.

Another NDT widely used in industries to verify the surface integrity of equipment is EMAT sensors [36]. These devices can emit and receive ultrasound on conductive metals without physical contact with the surface. The sensor utilizes a magnet to generate a static magnetic field and an electric coil to produce an alternating current magnetic field.

The ultrasonic waves for wall thickness measurements are generated with the interaction of both fields. Since the system operates without contact, the inspection of mechanical equipment utilizing EMAT sensors is recommended when the surface is inspected at high or low temperatures. Although the EMAT sensor does not require physical contact, some proximity between the sensor and the surface is required [15]. Figure 2.5 compares the technology utilized in UT and EMAT sensors.

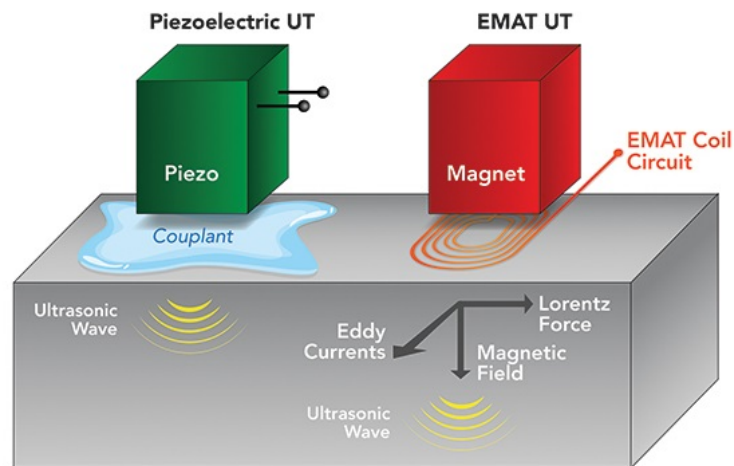


Figure 2.5: Technology comparison between UT and EMAT sensors [17].

Other electromagnetic techniques for inspection can be used. As an example, eddy current (EC) detects surface defects without contact, similar to EMAT sensors. The EC technique also utilizes a magnetic field to detect surface defects as cracks, corrosion, and heat deformations. Another example of electromagnetic use for inspections is the magnetic flux leakage (MFL). The MFL sensors are generally used in the petrochemical and material industries. The method can be applied to detect surface defects and wall thickness measurements. Many other non-destructive methods exist for surveying, however, they will not be discussed within this paper.

Human inspection using non-destructive techniques can be limited. Some industry equipment are inaccessible, such as those located in hard-to-reach areas or hazardous environments. Examples of these include buried pipes, power distribution lines, or superheater pipes. As an alternative for traditional human inspection, some robotic tools aim to cover the areas that humans cannot access. These robots commonly utilize ad-

vanced technology and non-destructive techniques to verify the integrity of industrial components. An overview of the most common types of robots is presented in the section below.

### 2.3 INSPECTION ROBOTS

The application of robots in the industry is not recent. They became popular a few decades ago, with the objective of automatizing processes and reducing production time. However, the use of robots for inspection purposes is a niche in the robotic industry due to constraints of the inspection. For example, some robots need to face degraded construction sites, while others have to inspect pipelines. Independent of the environment in which the robot is inserted, inspection robots have to overcome significant challenges and use modern technology to perform its task.

Regarding inspection capabilities, early robots offered visual feedback with the use of cameras. Most recent technologies bring multiple NDTs to improve the visual inspection offered by the pioneer robots [7]. The NDTs utilized can vary and change according to the demand for each system. For example, UT and EMAT sensors are used mainly in industrial robots to measure the wall-thickness of metallic and non-metallic materials. Some robots use LiDAR sensor to evaluate large structures such as bridges and buildings. Automated inspection systems involve a considerable range of robots that can be applied to different environments.

When analyzing systems capable of inspecting pipelines, the literature presents two distinct types of robots: external and internal systems. External systems crawl on the outside of the pipelines using different adhesion mechanisms and can detect pinholes, cracks, and thickness reduction due to erosion and corrosion. Internal inspection systems offer an alternative to the more conventional external approach. These systems do not have issues with the external constraints, but have their own challenges due to the reduced availability of space. An overview of these two systems is presented below.

### 2.3.1 EXTERNAL INSPECTION ROBOTS

Current research on inspection platforms has been focused on using robots to perform external inspection as an alternative to the manual method. These systems use different mechanisms to hold onto the outer wall of pipes and use NDTs to validate the integrity of the tubes. However, the robotic platform experiences some challenges while performing the inspection. As an example, the tubes can be located in hard-to-reach areas or have limited space between them. The surface of pipes may also be irregular and degraded. Furthermore, the presence of features such as elbows, valves, and bends add more complexity to the environment faced by the robot.

Various applications of robotic technology have led to the development of new locomotion concepts. One of these is the ability to climb on pipes using magnetic components [42, 16]. The mechanisms work by creating an opposing force onto metallic walls using a permanent magnet or electromagnet. Badokar et al. [6] describes a magnetic system developed for the Bhabha Atomic Research Centre for the inspection of superheater tubes. The system uses caterpillar traction to move along the pipes and is equipped with an EMAT sensor to perform wall thickness measurements. Figure 2.6 show the robotic platform during pipeline inspection of superheater tubes.

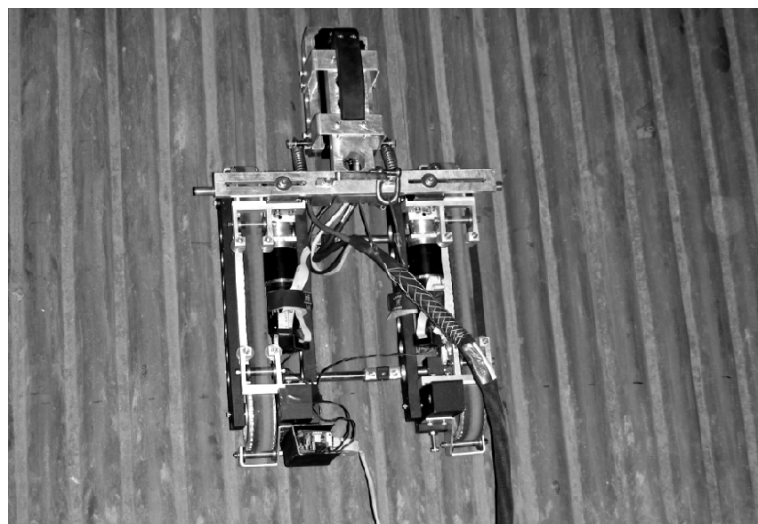


Figure 2.6: Robotic platform with magnetic caterpillar traction system [6].

The use of magnetic wheels is also introduced in the literature. Tavaloki [45] describes a robot with omni-directional wheels for ferromagnetic structures. The robot utilizes a magnetic core to crawl on vertical pipes and can be adapted for flat and curved surfaces.

As an alternative for non-metallic surfaces, robots that use suction [27], or attraction force generated by propeller [32, 5, 4] have been used. They have the advantage of holding onto ferrous or non-ferrous surfaces. The propeller system generates a normal force using engines and propellers to create thrust. The normal force generated against the surface adheres the platform to the surface. This mechanism allows the robot to navigate into different materials and pass over different obstacles.

Nishi [32] describes a propeller robot with its movements controlled by the motor's revolution speed. Ali et al. [4] also utilizes a propeller to maintain the robot steady to the wall. However, instead of controlling the platform with revolution speed of the propellers, Ali proposes a movement generated by electric motors attached to wheels. The robot, shown in Figure 2.7, utilizes a UT sensor to take wall thickness measurements of superheater and petrochemical tubes.

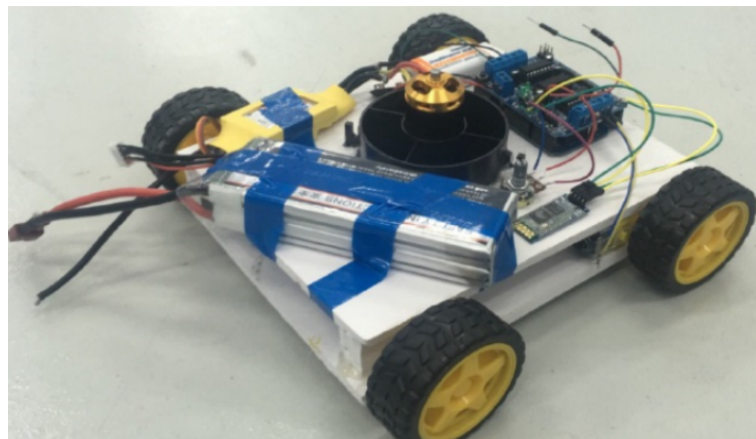


Figure 2.7: Robotic platform with propeller system [4].

Suction robots hold onto the surface by producing a negative internal pressure within a sealed area between the surface and the robot. Small discontinuities in the environment such as screws or solder traces can prevent complete sealing, leading to a failure in the suction system. This mechanism is ideal for clean and even surfaces and few studies

could be found for application on small-diameter pipelines. Example of suction robots include the Alicia climbing robot [27]. The robotic platform utilizes a suction mechanism on its core and navigates on the surface with the use of wheels. The robot can overcome discontinuities up to 1 cm and has a payload of 8 kg.

Another locomotion approach presented in the literature and used in the industry is gripping robots, which hold onto the surface with the use of clamping mechanisms. The platform presented by Choi [11] has two grippers and a motorized core to navigate on the pipe surface. Industrial applications for this locomotion mechanism include the remote-controlled scanner HydroFORM [23]. The robot utilizes sensors and a camera to perform surface mapping and wall thickness measurements. Figure 2.8 shows the HydroFORM performing a field inspection with the assistance of an operator.



Figure 2.8: HydroFORM inspection tool [23].

Although some of the technical issues with external systems have been addressed, there are still some challenges that need to be investigated. These include the potential difficulty of navigating on pipes with limited external access as the tubes are often close to each other. The tubes inside the combustion chamber of fossil fuel powerplants are an example of a pipeline with limited external access.

### 2.3.2 INTERNAL INSPECTION ROBOTS

The literature has introduced several designs for in-pipe inspection robots. Variations in pipeline geometries have contributed to the development of innovative concepts in locomotion. One of the most essential considerations in the design of a robotic platform is how to obtain the necessary traction force for it to move along a surface. Based on the mechanical architecture, internal pipe inspection systems have been classified by Deepak et al. [12] into six different categories, as shown in Figure 2.9.

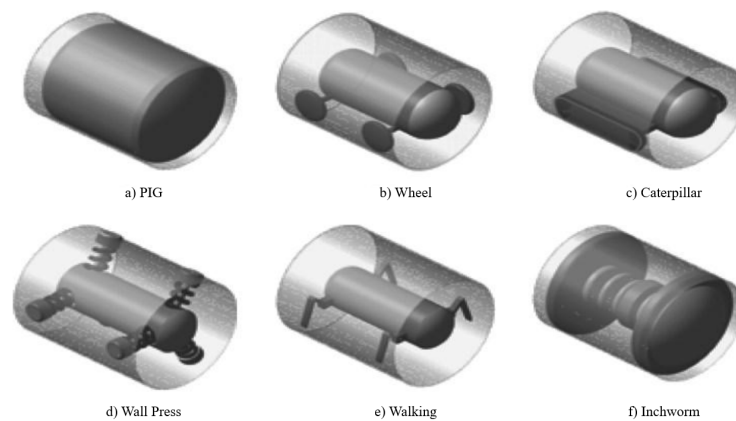


Figure 2.9: Mechanical architecture of internal inspection robots. Adapted from Choi and Roh [41].

One of the most commonly used systems for pipe inspection is the pipeline inspection gauge (PIG) [7]. The locomotion system of PIGs utilizes fluid pressure differential to drive the robotic platform through the tubes. However, in the presence of elbows, T-junctions, or bends, the system is limited and cannot be used. These pipelines are commonly named unpiggable pipelines.

PIGs have been used in various industrial sectors since they were first invented. Each platform is designed to inspect and clean different pipe diameters. Guan et al. [20] utilizes a multi-sensor intelligent PIG for surveying small-diameter pipelines. The PIG developed by Guan addresses the various requirements of small pipeline inspection with the use of several sensors as IMU, optical sensors and an MFL sensor.

Another type of traction system is the wheeled type [47, 19], which provides great steering capacity and high-speed mobility. The motion is usually generated by electrical

motors attached to wheels. They can be combined with other suitable traction methods such as wall press and magnets for improved traction. Figure 2.10 show a wheeled robot with wall press mechanism.



Figure 2.10: Wheeled type robot [30].

Wheeled systems are classified as the primary locomotion method for internal pipe inspection robots. Dertien et al. [14] utilizes a set of v-shaped omni-wheels in his robot to generate traction. The system carries a camera and an additive noise-based sensor to detect leaks on low-pressure gas distribution. An example of wheeled robots with wall-press mechanisms is presented by Kim [25]. The robotic platform utilizes expansion and clamping mechanisms to hold the pipe wall and can be adapted for different pipe diameters.

As an alternative, tracking systems, also known as caterpillars, can be used in place of wheels. This mechanism provides a better friction force due to the larger contact area. Caterpillar robots can also utilize wall press mechanisms for improved traction within the tubes [29].

The Famper robot from Seoul National University [18] is a robotic platform developed to explore pipelines that use traction systems with wall-pressing mechanisms. The robot is built with four separate tracks that actuate independently to allow the robot to drive through obstacles. Another example of a caterpillar system, developed in Hanyang

University [26], contains a two-part mechanism that allows a robot to wall-press using a passive adaptation module and differential steering. The system developed at Hanyang University (Figure 2.11) can handle various in-pipe obstacles such as T-joints and bends.

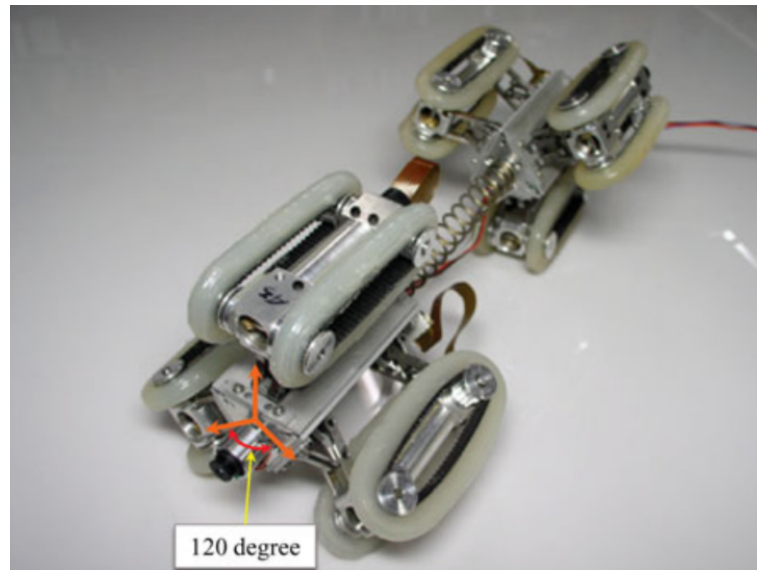


Figure 2.11: Caterpillar robot [26].

The literature also presents walking robots for in-pipe inspection. These robots are usually complex and extensive in size due to the large number of actuators required to generate motion. Their mechanisms generally make them slow to navigate inside the pipe [29]. Little research could be found of robotic systems that use walking platforms for navigating inside small-diameter the pipelines.

Examples of walking robots in the literature are introduced by Yu et al. [49], who proposes a novel walking robot that can adapt to different pipe diameters. The robot utilizes a system of planetary and sun gears to navigate into the pipe. Although these systems are not commonly used in the industry, they most often include features to overcome specific project requirements.

Inchworm in-pipe robots [8, 39] generally use peristaltic motion to navigate through the pipeline using mechanisms such as grippers and extenders. The gripper enables the robot to attach to the tubes' inner walls, making a constant normal force. In sequence, the extender can expand and contract in a sequential series, generating motion. Inchworm

robots are generally more stable than other designs and can navigate on vertical and horizontal pipelines.

These robots typically use electrical motors or pneumatic actuators to generate motion. Ono et al. [35] introduces an example of a pneumatic earthworm robot. The system utilizes a vacuum tank and air compressor controlled by a computer to provide a means for the robot to navigate. The robot is modular and moves at a velocity of 13 mm/s. As an alternative to pneumatic actuators, Yousef et al. [48] introduces a inchworm robot that can adapt for different pipe diameters. The robot uses gripper and extender modules powered by electrical motors to navigate in the pipeline.

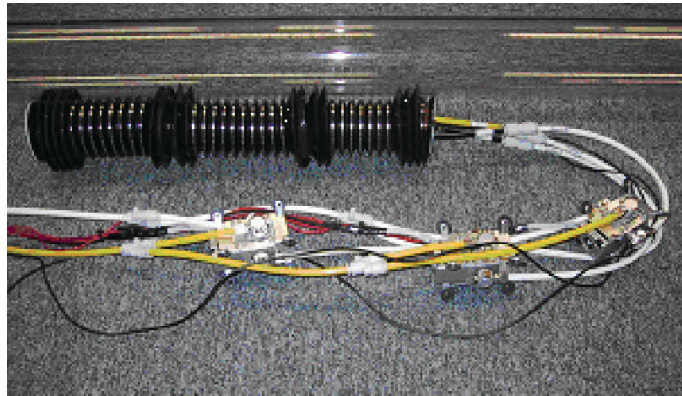


Figure 2.12: Inchworm robot [35].

In general, there has been little research conducted on the development of internal pipe crawlers for small diameter pipes that are typical of superheater tubes. This is likely due to the limited space available and the coiled nature of the tubes. This research effort aims to create a novel robot for application in this environment. The proposed platform is presented in Chapter 3.

### 3. SYSTEM DESCRIPTION

Robotic platforms using NDTs to increase the reliability of inspections are a requirement for today's industry demands. This chapter introduces the concept of an automated tool for the inspection of superheater pipes to meet this demand.

#### 3.1 GENERAL SPECIFICATIONS

The state-of-the-art of inspection robots has presented several locomotion concepts for pipeline inspection. However, none of the systems discussed in Chapter 2 can navigate through multiple sharp bends in a 50.8 mm pipe, which is critical for the robot to inspect superheater tubes effectively. The prototype design focused on the robot's capability in maneuvering through 90° and 180° bends commonly found within the pipeline of superheater tubes. Figure 3.1 shows two bend curvatures on 50.8 mm pipe with a wall thickness of 2 mm.

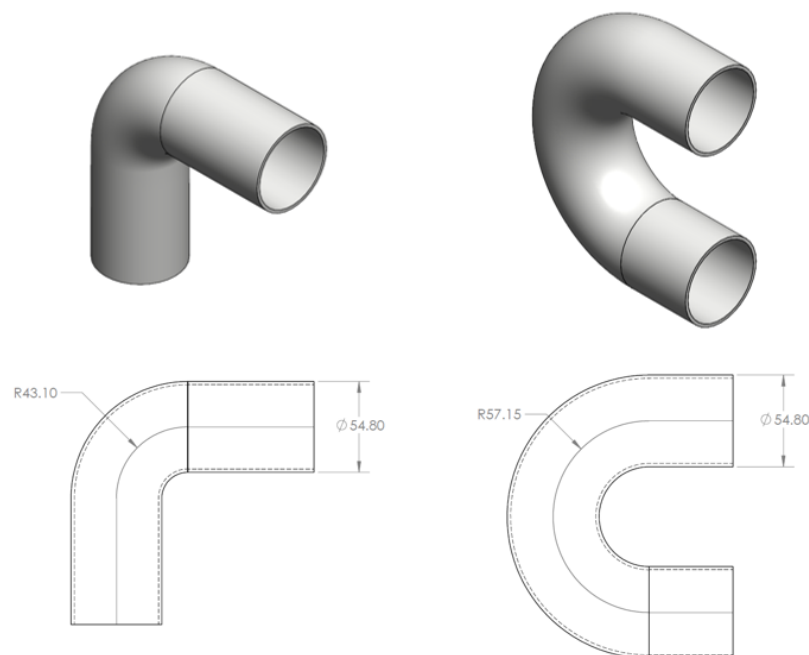


Figure 3.1: Schematic of the pipe elbows.

### 3.1.1 LOCOMOTION SYSTEM

The opportunity to reduce costs and increase the reliability of inspections has led to the development of several designs for inspection robots. They have different mechanisms to generate traction within the tubes and aim to verify the integrity of the pipeline.

Designing a platform to inspect the pipe's integrity can be arduous if made from the exterior. The tubes in the combustion chamber of fossil fuel powerplants can be close to each other, providing minimal spacing in between. Moreover, the coiled structure of the pipeline makes it challenging to design an external inspection robot.

Inspecting the superheater pipes from inside offers an alternative to the external approach. Some challenges on inspecting the pipeline from outside are addressed with in-pipe robots; however, these mechanisms face different constraints. For example, the interior of superheater tubes can contain moisture and material deposition and can be irregular due to thermal expansion. Therefore, choosing an adequate locomotion system is critical for the success of the project.

Among the locomotion systems commonly used, the limited access to the tube restricts the use of PIGs. Wheeled or tracked systems can slip inside the tubes and generally do not have high pull force capabilities. Space availability inside the 50.8 mm pipe restricts walking robots, commonly used in larger diameter pipes. The inchworm type is the locomotion system that can adapt better to the coiled tube structure. These robots also have advantages over the other locomotion systems for small diameter pipes.

Inchworm robots utilize peristaltic locomotion, similar to earthworms that travel by contracting their body segments sequentially, as illustrated in Figure 3.2. This system generally has great pull force capabilities and can navigate on vertical and horizontal pipelines.

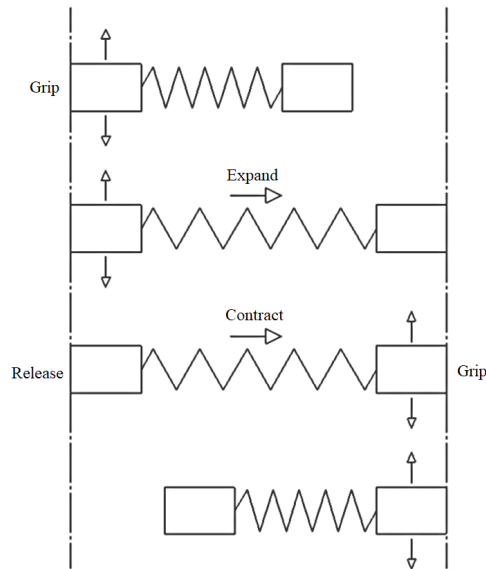


Figure 3.2: Peristaltic locomotion of the robotic crawler.

### 3.1.2 KINEMATIC ANALYSIS

Each module's dimensions must be determined to ensure that the robot can successfully navigate the 5 cm tubes and maneuver through the bends. Figure 3.3 highlights external parameters that limit the module's size, such as bend radius ( $R$ ) and inner diameter of pipes ( $D$ ). The parameters defining the module's geometry are length ( $H$ ) and width ( $W$ ).

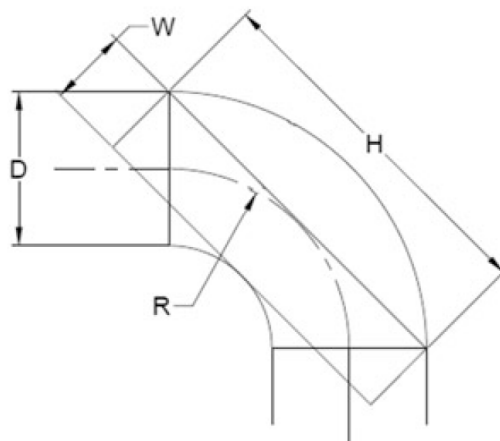


Figure 3.3: Parameters to determine the module's size [34].

Two distinctive approaches can determine each module's geometry. Figure 3.4 illustrate the two cases where the module's length (case 1) or width (case 2) can be greater

than the optimal geometry ( $W$  and  $H$  from Figure 3.3). If any of these situations occur, changes on the module's dimensions are needed to ensure that the crawler can maneuver through the  $90^\circ$  bend.

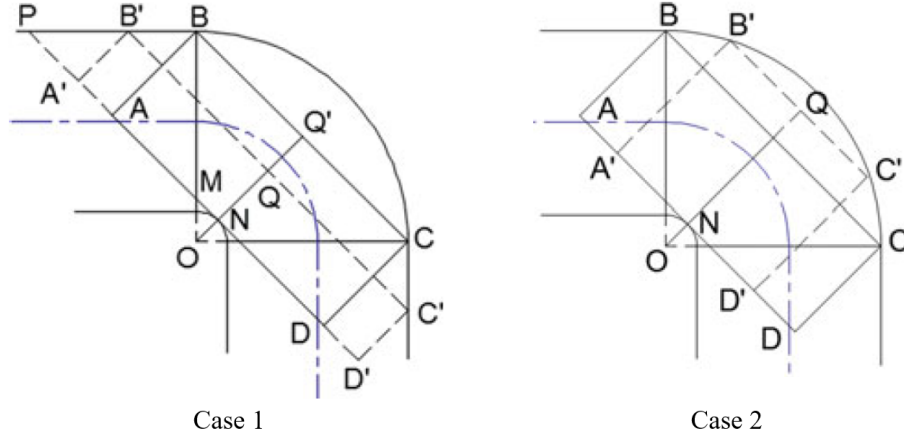


Figure 3.4: Diagram illustrating changes on the length (case 1) and width (case 2) for the robotic module [34].

Case 1 occurs when the robot's length ( $A'D'$ ) is greater than the optimal length ( $AD$ ) and a reduction in the module's width ( $A'B'$ ) is necessary. In case 2, when the width of the module exceeds the optimal width ( $AB$ ), the module's length has to be reduced. Equation 3.1 defines the optimal width for the module.

$$AB = \left[ \left( R + \frac{D}{2} \right) \cos(45) - \left( R - \frac{D}{2} \right) \right] \quad (3.1)$$

The robotic crawler developed must be capable of navigating in tubes with an internal diameter of 50.8 mm. The bend radius commonly found in superheater tubes and used for determining the module's geometry is 43.1 mm. Solving Equation 3.1, the optimal width for the module is found to be 30.7 mm. Equation 3.2 is used to determine the optimal length for the robot's modules.

$$AD = 2 \times \sqrt{\left( R + \frac{D}{2} \right)^2 - \left( R - \frac{D}{2} + (AB) \right)^2} \quad (3.2)$$

The optimal length for the module is 96.9 mm, calculated using Equation 3.2. However, a desirable shape for the robotic module is cylindrical with 70 millimeters in length

and 35 millimeters in diameter. Thus, the diameter of the module exceeds the optimal width of 30.7 mm. In this context, Equation 3.3 is used to verify if a module with the dimensions desired can pass through the bends.

$$A'D' \leq 2 \times \sqrt{\left(R + \frac{D}{2}\right)^2 - \left(R - \frac{D}{2} + (A'B')\right)^2} \quad (3.3)$$

Using the desirable value for the module's diameter, the maximum length calculated with Equation 3.3 is 87.5 mm. Since the value desired for the module's length (70 mm) is lower than the calculated value (87.5 mm), the desired module's geometry will be able to maneuver on the 90° bends. Analysis shows that modules with a 35 mm diameter and 70 mm length can also maneuver 180° bends. Furthermore, on each module's front and back caps, a tapered section of 10 mm (length) by 15 mm (diameter) can be used to provide extra space without hindering the module's turning ability. Figure 3.5 demonstrates the kinematic evaluation of a module on a 180° bend (the values in Figure 3.5 are in millimeter).

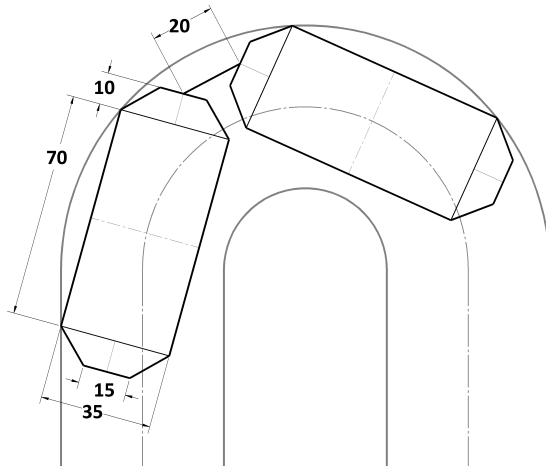


Figure 3.5: 180° bend kinematics.

### 3.1.3 ACTUATORS

The selection of actuators has a significant impact on the design of the inspection tool. Previous crawlers introduced in the literature use pneumatic pistons and valves to produce movement. These components provide a simple means of producing motion with

the use of compressed air. However, the drawback for the system is the necessity of connecting two air tubes necessary to expand and contract the pistons on the module. Together, the tubes make a thick and rigid tether. Furthermore, obtaining miniature off-the-shelf pneumatic components for the module's constrained space proved to be a challenge.

An alternative to the pneumatic actuators is the use of electric motors. A number of options are available on the market and different configurations of reduction rate, input voltage, and stall torque can be found. Moreover, several types and dimensions are commercially available, making them suitable for different projects. Two different types of motors are utilized in this research effort. These are metal (a) and plastic (b) gear motors as shown in Figure 3.6.

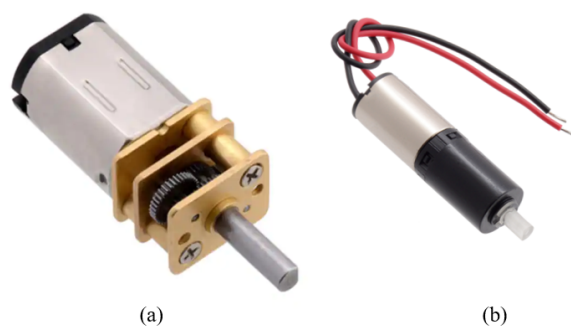


Figure 3.6: Electric motors.

These motors require direct current power provided through a tether and operate at different voltages. The small plastic gear motor has an input voltage of 3 to 6 V and is offered with four different reduction rates. It has a diameter of 6 millimeters and the stall torque varies from 22 to 900 g.cm. The metal gear motor operates at 12 V with a maximum current of 1.6 amperes. Its cross-sectional area measures 10 x 12 mm and different gear ratios are offered, with a wide range of torques provided.

### 3.2 PERISTALTIC MODULES

Movement of the crawler is generated using a set of gripper and extender modules that propel the crawler forward using peristaltic motion, similar to earthworms that travel

by contracting their body segments sequentially. Each module holds a linear actuator consisting of a rotating lead screw and nut. The basic design is composed of five modules: two grippers, one at the front and one near the rear of the system, two extenders between the grippers, and one electronics module. The peristaltic movement of the crawler is shown in Figure 3.7.

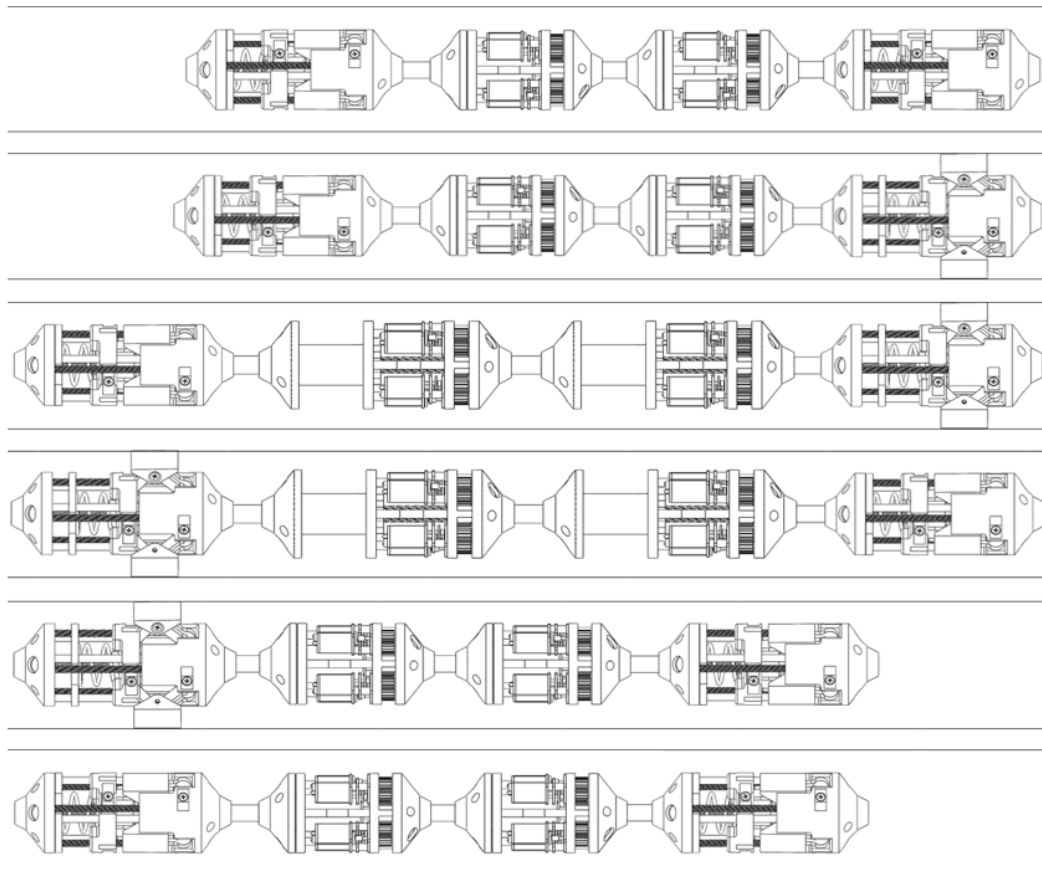


Figure 3.7: Peristaltic motion of the crawler.

Each gripper contains linkage arms that push small pads radially outward and engage the inner pipe wall. The radial symmetry of the design allows for three sets of linkage arms and gripper pads. These linkages are driven by a mechanism attached to the nut of the rotating lead screw. Similarly, the extenders utilize a nut at the center of the module, which expands and contracts. The movement of the modules are repeated sequentially, generating motion for the crawler.

### 3.2.1 GRIPPER MODULE

The gripper module has three pads to hold into the pipe wall. The pads are connected to a moving disk and the module's base. The moving disk has a central hex nut, which transforms the rotational movement of the lead screw to the linear movement of the disk. The pads open and close perpendicular to the tube wall with the movement of the disk. A metal gear motor installed on the module's base actuates the lead screw. Figure 3.8 shows the components of the gripper module.

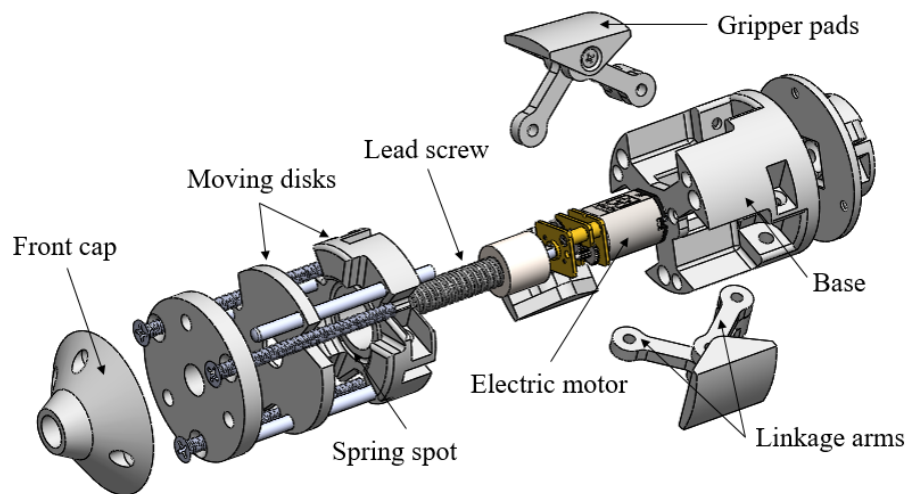


Figure 3.8: Gripper module.

Instead of having a single moving component that contains the nut for the lead screw and the linkages for the gripper arms, the two functions were split into two moving disks connected by a spring. The mechanism allows the pads to continue exerting force on the pipe while the motor is off. In addition, this was designed to prevent the motor from stalling before the gripper arms lock into the pipe wall. As a result, when the pads are forced to stop moving outwards, the moving disk with the nut can continue its motion towards the fixed disk, compressing the spring and, increasing the current on the motors.

The mechanism can extend past the pipe wall, allowing for variations in pipe diameter. Additionally, the pads are covered with rubber for increased friction. All the parts of the crawler were 3-D printed and assembled using off-the-shelf components as

screws, dowel pins, heat sets and the electric motors. Figure 3.9 shows the preliminary prototype.



(a)



(b)

Figure 3.9: Assembled gripper module with pads closed (a) and opened (b).

### 3.2.2 EXTENDER MODULE

The extender module utilizes a lead screw to generate the linear motion required for the peristaltic movement. Two electric motors drive the lead screw and these components are connected by a set of gears located on the module's base. A cylinder holds a hex nut that transforms the rotation of the lead screw to linear movement to the cylinder. The cylinder then propels the front cap of the module, generating the motion. Dowel pins guide the cylinder and its end-stop is given by a disk fixed to the module's base by screws. Figure 3.10 shows the design of the module, highlighting some of its components.

The reduction rate of the motors and the travel distance per turn of the lead-screw directly affect the crawler's velocity and pull force capabilities. Therefore, the optimal

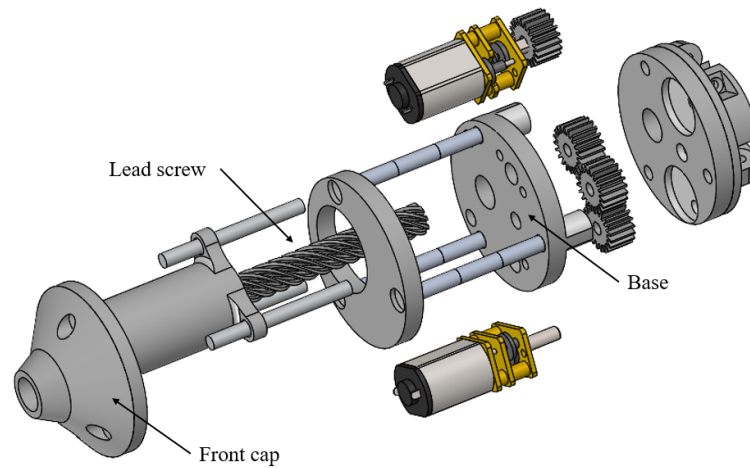


Figure 3.10: Schematic of the extender module.

combination of those components lead to an increased payload and faster travel per cycle. Several combinations of motors and lead-screw were tested during the development of the module. The one that best facilitated the projects' requirements used a reduction rate of 298:1 for the electric motor and the fast track-lead screws with a travel distance of 8.45 mm per turn. Details about the speed and pull force capability of the crawler are presented in Section 4.

The extender module utilizes some metal components to increase the overall accuracy. As an example, the metal gears fit without any gaps. This efficiency would be difficult to achieve by 3-D printing such small components. Other metal components being used include dowel pins, heat-set, and the lead screw. In addition, a small printed circuit board (PCB) was designed to Y-cable the electric motors. The board also assists in replacing the electric motors if a malfunction is detected. Figure 3.11 shows the module assembled with the PCB attached to an electric motor.

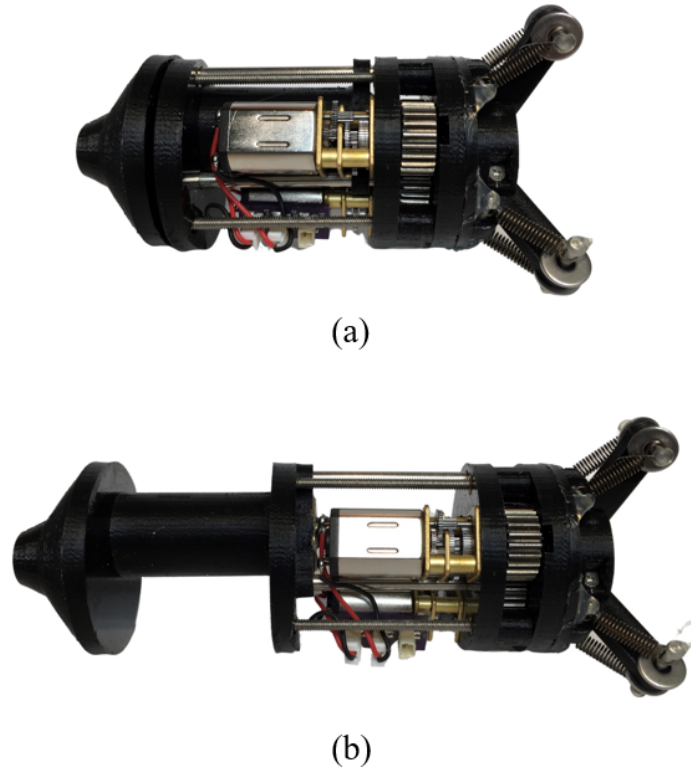


Figure 3.11: Assembled extender module in contraction (a) and expansion (b).

### 3.2.3 ELECTRONICS MODULE

The electronics module holds the sensors and microcontrollers necessary for controlling the electric motors that generates the peristaltic movement. Several options have been considered for the module's control tool. The first included building an arrangement of breakout boards stacked together inside the front cap of each module. However, due to the constrained space, the off-the-shelf electronics board proved to be sizable, restricting its utilization.

Creating another module to hold the sensors was an alternative option. The module design contains four panels to mount the electronics. A PCB was developed to simplify the soldered connections and wiring. A microcontroller, current sensor, and motor drivers were used to control the movements of the crawler. These components communicate between themselves through I2C communication protocol. A challenge when developing the electronics module was the compact arrangement of the wires. Therefore,

efforts were focused on designing the boards with plastic JST connectors to minimize the module size. Figure 3.12 shows the electronics module highlighting the components used for controlling the peristaltic crawler.

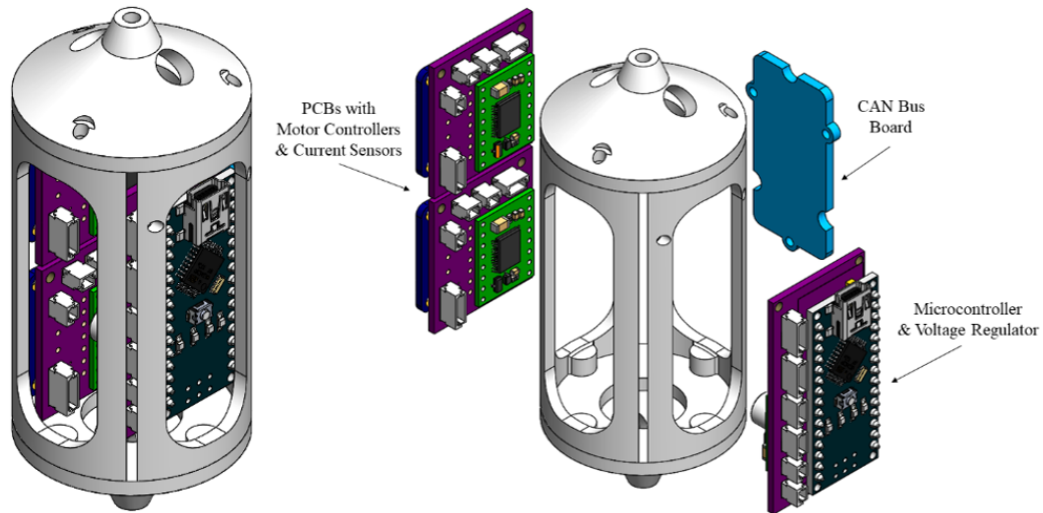


Figure 3.12: Electronics module.

### 3.3 INSPECTION MODULES

The purpose of the crawler is to provide information regarding the structural integrity of key pipeline components in fossil energy power plants. Additional modules have been developed to house inspection sensors and are described in the following subsections.

#### 3.3.1 INSTRUMENTATION MODULE

The instrumentation module is designed to improve the inspection tool capabilities, robustness, and operational feedback. The module consists of a rotative cylinder with a stationary top and bottom flanges. This module utilizes a spur gear mechanism to provide the rotation of the cylinder, which constantly spins 360° degrees concentrically about the center of the tube. Six plates are attached to the cylinder wall and each plate accommodates different sensors to evaluate the conditions of the tube. Each panel design can be modified to support a different sensor, varying according to each project's

necessities. Figure 3.13 shows the module’s rotating drum and the motor housing, highlighting some of its components.

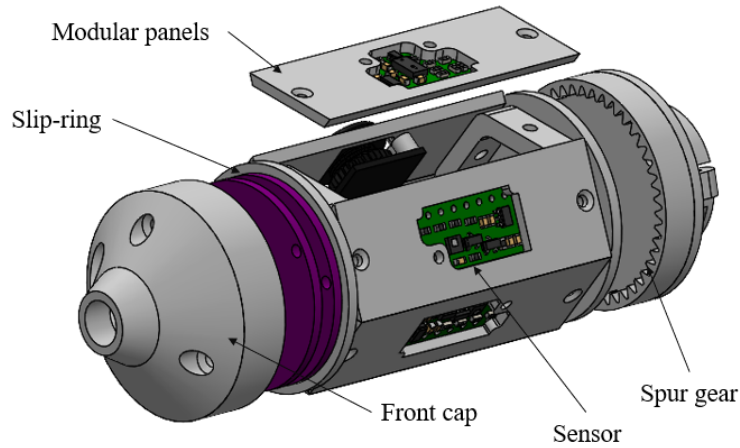


Figure 3.13: Schematic of the instrumentation module.

The module currently includes 3 sensors for assessing the tube conditions. The three current sensors include an analog video camera, an environmental sensor for temperature and pressure measurements, and a LiDAR sensor. The LiDAR can provide information on potential surface anomalies and defects. An inertial measurement unit (IMU) is also included in the module and provides the angular position and acceleration of the crawler. Table 3.1 shows the specifications of the sensors currently installed in the module.

Table 3.1: Sensor specifications.

Sensor	Measurement	Range	Resolution	Unit
Environmental	Temperature	-40 – +85	±1	°C
	Pressure	26 – 126	±0.02	kPa
IMU	Acceleration	±2 – ±16	±0.004	<i>g</i>
	Angular Velocity	±125 – ±2000	±10	°/s
Camera	Surface Imaging	640X480	VGA	Pixel
LiDAR	Circumferential Mapping	10 – 60	±1	mm

A PCB embeds a microcontroller and a motor driver to manage the communication within the module sensors. The PCB designed uses I2C communication between the sensors and the microcontroller and incorporates JST wire connectors. The use of components available on the market includes the M2 screws and spacers that maintain the unit's rigidity. Furthermore, bearings were placed between the drum and the flanges (top and bottom) to reduce friction between the moving components. Figure 3.14 shows the module assembled with its front-cap opened.



Figure 3.14: Instrumentation module assembled.

A slip-ring was developed to improve the wire management during rotation. The mechanism consists of a round PCB in the form of a disk. It utilizes the radial direction to connect two disks with exposed wires of varying radius. A flexible copper wire with a miniature metallic spherical tip connects the power and signal tracks and the brush block. The system is integrated into the front end, while the spur gear is attached to the back. This mechanism is commercially available and a range of different diameters and types was found. Although, an off-the-shelf slip ring to fit inside the 35 mm module could not be found. Figure 3.15 shows the design created and the rings' exposed wires with the spinning copper cables soldered onto the board.

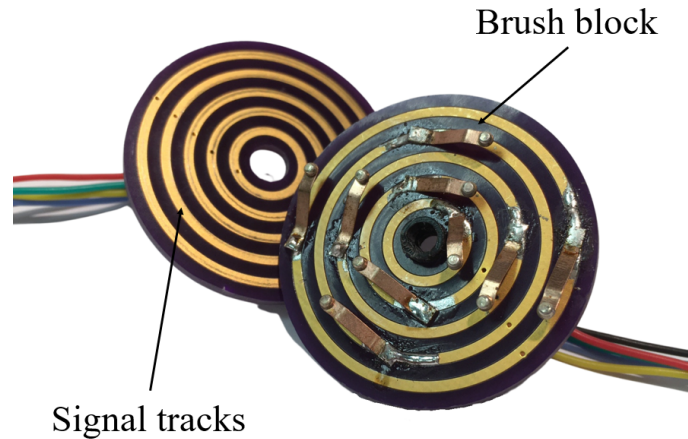


Figure 3.15: Slip-ring.

### 3.3.2 UT SENSOR MODULE

The module design allows the UT probe's accurate positioning into the pipe surface, providing repeated wall thickness measurements. A linear actuator mechanism allows for the prismatic movement of the probe inside the pipe. The mechanism utilizes two plastic gear motors connected to a gearbox and a lead screw. The lead nut is attached to a housing for the UT sensor and translates along the lead screw, converting the rotary motion from the motors to a linear motion for the sensor. A spur gear system was added to the module to allow wall thickness measurements at different circumferential spots. A stationary spur gear was mounted on the front end of the module and acts as the output shaft. The input shaft gear, connected to a plastic gear motor, spins with the module. A set of bearings permits the rotation and reduces the friction between the moving parts. This mechanism provides a full 360° rotation of the modules and allows the UT sensor to measure the tube thickness at any radial location. A schematic of the module highlighting the major components is shown in Figure 3.16.

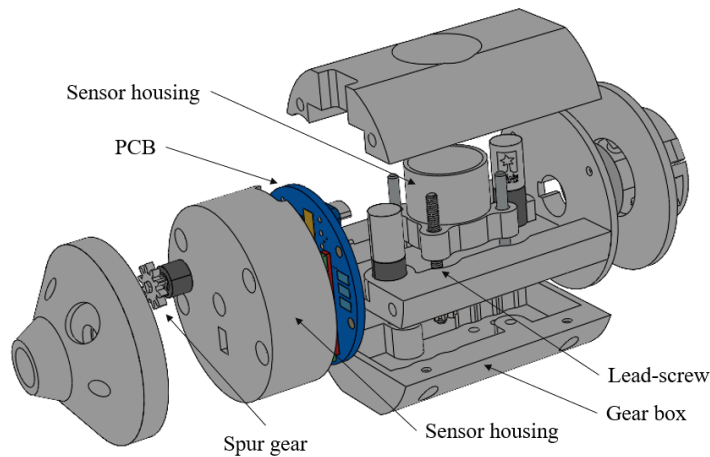
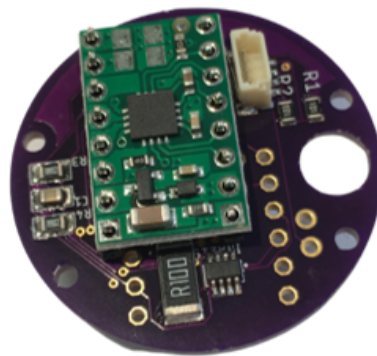


Figure 3.16: Schematic of the ultrasonic transducer module.

During the development of the UT sensor module, PCBs were adapted to the constrained 35 mm diameter of the crawler. As a result to maximize spacing for the electronics, the boards were designed to be circular. This architecture allows the circuit board to be positioned concentric inside the module, saving space compared to the traditional rectangular boards. In addition, the design contains a 6 mm hole to allow an electric motor to pass through the other side of the PCB. This motor is used for rotating the spur gear positioned at the front cap of the module and providing 360° rotation for the module. The PCB designed improved the integration between the UT Sensor with the other modules. This board contains a microcontroller, a dual motor controller, and a current sensor. The PCB also contains a serial port for CAN Bus communication with the electronics module and an external control box. The front-end of the unit contains an electronics cover where the PCB is attached. Figure 3.17 shows the module assembled and the PCB with a current sensor microchip embedded to the board.



(a)



(b)

Figure 3.17: UT sensor module (a) and PCB (b).

### 3.3.3 SURFACE PREPARATION MODULE

The UT sensor probe requires a fluid couplant to remove the small air gap between the probe and the tube wall and the surface of the pipe may need some cleaning in order to obtain accurate measurements. Therefore, a separate module was developed for the integration of the UT couplant and a surface-cleaning brush. The module design contains four motorized components: a surface brush, a couplant pump, a linear actuator, and a spur gear mechanism.

The couplant is applied to the surface with a motorized peristaltic pump that controls the liquid flow rate. The module houses a reservoir containing enough couplant for multiple measurements of the UT probe. To clean the pipe surface, a brush is attached to

a motor, providing constant rotation to the brush. The cleaning mechanism is protruded and contracted by a linear actuator, which utilizes a plastic gear motor and a lead screw connect by gears. The mechanism allow for the the rotating brush and the peristaltic pump tube protrude and contract within the pipe. The module's rotation is given by a spur gear mechanism attached to the front end. Figure 3.18 shows the design of the module highlighting its components.

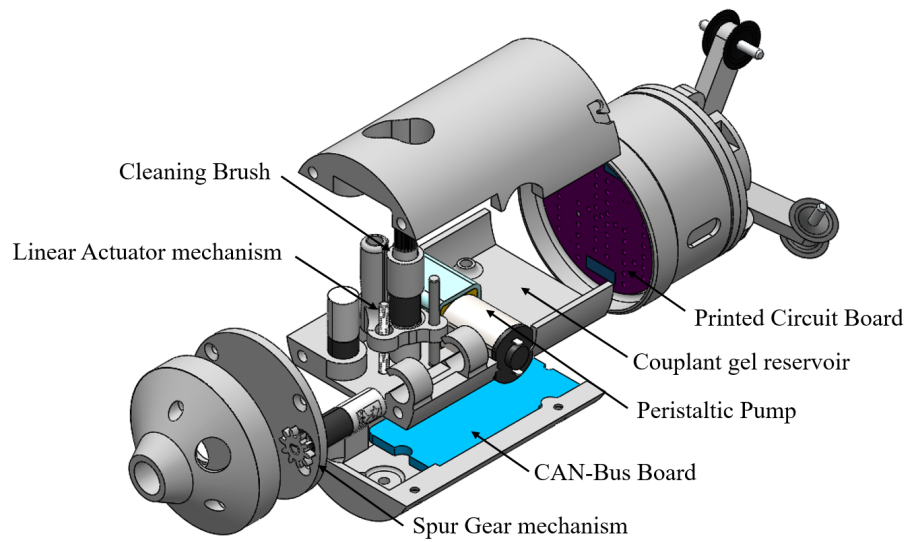


Figure 3.18: Schematic of the surface preparation module.

The surface preparation module also houses a PCB for control and communication of the mechanisms of the module. The printed circuit board connects an embedded microcontroller and two dual motor drivers. The board permits control of all four motors independently and allows for communication to the control box outside the tubes. An image of the assembled module is shown in Figure 3.19.



Figure 3.19: Surface preparation module.

### 3.4 SYSTEM INTEGRATION

The peristaltic modules go in front of all the inspection units, pushing them forward. The instrumentation module is located in front of the surface preparation and UT sensor modules. This design allows for the surface to be prepared prior to the UT sensor performing the inspection.

#### 3.4.1 STABILIZATION MECHANISM

A stabilization system was designed to maintain balance during circumferential rotations. It incorporates a set of lever arms mounted on three separate linkages, which are connected to a pair of springs providing consistent opposing force to a set of wheels, mounted on the outer extremity of the arm. The applied force offsets gravity during the rotation of the module, establishing continuous surface contact for each of the wheels during rotation. This mechanism allows the module to conform to the pipe surface in minor irregularities while maintaining precise placement. Figure 3.20 shows the stabilization mechanism designed.

A high resistance flexible tube attached to the rear end of each module provides the stiffness required but is also flexible enough to allow movement around the bends. In addition, the rear stabilization system provides enough stability for the module it is



Figure 3.20: Stabilization mechanism.

attached to and the unit following it. This allows both units to remain centered within the pipe. The tubes also house the wiring required for power and signal lines.

### 3.4.2 COMMUNICATION SYSTEM

The controller area network (CAN) is the serial protocol communication used for communication between the modules of the robot and the controller outside the tubes. CAN Bus is a messaging protocol based on pairs of receivers and transceivers and is especially useful for systems with multiple controllers. This serial communication is commonly used in automobiles and has fast-speed communication between the master and slave boards. In addition, this communication protocol was chosen for its debugging features and error management. The wires connecting the CAN Bus boards to the system include CAN High and Low for bi-directional data transfer and RX/TX to the Arduino microcontroller. Figure 3.21 shows the CAN Bus architecture.

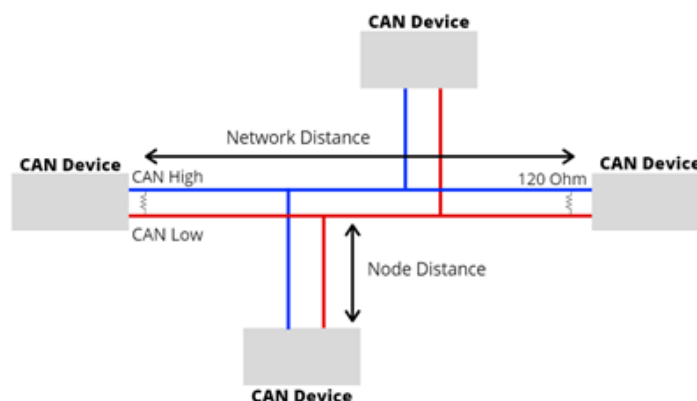


Figure 3.21: CAN Bus architecture.

The tether connecting the modular crawlers is a significant component of the system. It wires the multiple devices together in sequence, daisy-chaining all components, establishing intermodular communication, supplying electrical power, and providing video feedback to the controller outside the tubes. The tether contains wires for the power and ground lines and an analog video for transmitting images from the cameras. The CAN Bus communication requires two more wires on the tether for transmitting signal. The PCB design on each module considered the wiring for the tether and JSTs were used for connection within the board. The design of the tether system is shown in Figure 3.22.

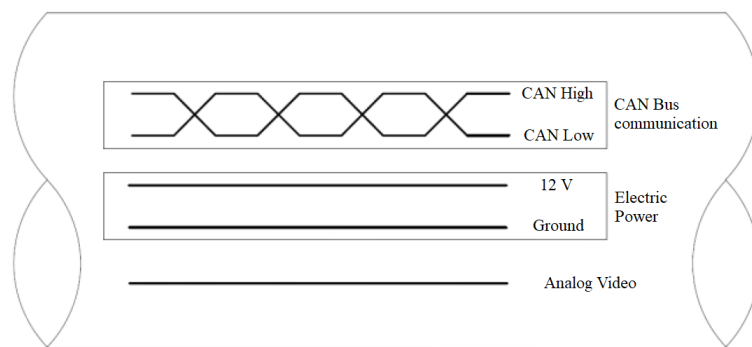


Figure 3.22: Tether configuration for the crawler system.

## 4. TESTING

The process for developing the robotic crawler included evaluating initial concepts, prototyping, bench-scale, and engineering scale testing. This chapter focuses on the testing aspects used to validate the concepts and demonstrates that the system can navigate through multiple bends and straight sections.

### 4.1 BENCH SCALE TESTING

To validate the crawler's performance when navigating through bends and straight sections, several tests using small sample pipes were performed during its development. The tests assisted in defining optimal parameters such as the reduction rate of the electric motors and the travel distance per turn for the lead screw. Tests were also performed on the inspection modules to evaluate their ability to measure the wall thickness of pipes, detect imperfections using the LiDAR sensor, and their communication capabilities.

#### 4.1.1 PERISTALTIC CRAWLER

To evaluate the pull force capability of the crawler, pull force tests were conducted on the gripper and extender modules. The grippers were found to be capable of pulling approximately 84.5 N of force and the extenders were found to generate 40 N of force. The pull force tests were conducted using a digital weight scale attached to the ends of the modules. The value for the gripper was found by finding the maximum pull force before the gripper pads began to slip along a steel 5 cm diameter tube. The pull force for the extender was found by clamping the module to a flat surface and allowing the linear actuator to pull the scale.

Tests were also conducted on the crawler prototype in a straight pipe section to evaluate the overall speed with the fast-track lead screw as well as to validate the automated module movement controlled by the current sensors. The crawler moved approximately

30 centimeters in 1 minute, which is significantly faster than the initial prototypes. Figure 4.1 shows the crawler successfully navigating inside the acrylic pipe.

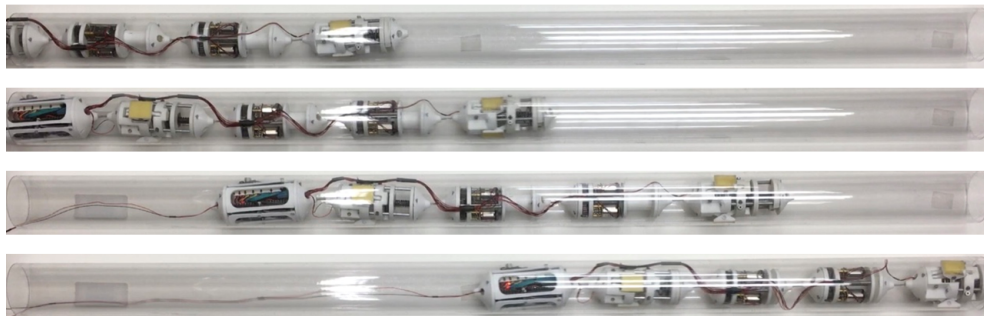


Figure 4.1: Robotic crawler traveling in straight tube section.

Another bench-scale test was conducted for testing the crawler's ability to navigate through a 180° bend. A custom built rigid clear pipe with a 7 cm bend radius was used for the testing. Efforts were made to purchase even smaller bends, replicating an actual boiler tube curvature radius, however, the 7 cm bend radius was the smallest that could be applied to the material for a continuous 50.8 mm interior. During testing, shown in Figure 4.2, the crawler was successfully able to navigate around the acrylic bend in approximately 1 minute.

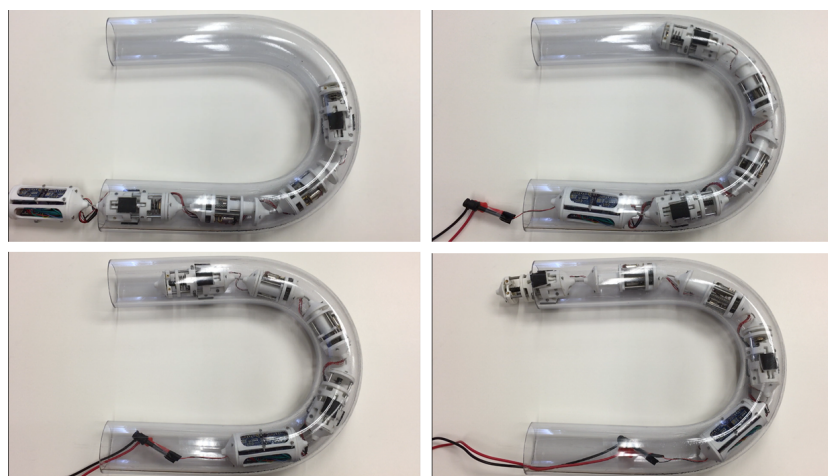


Figure 4.2: Robotic crawler traveling in a plastic 180° bend.

#### 4.1.2 INSTRUMENTATION MODULE

To assess the scanning capability of the instrumentation module, a 3-D printed template ring was used to simulate a 5 cm diameter surface with a variety of irregularities. For the tests, the module is positioned at the center of the template frame and rotated to scan the surrounding irregularities on the ring. Figure 4.3 shows the template ring and the instrumentation module positioned at the center, as well as the results obtained. Note that the data acquired was scaled to match real values and filtered for better visualization.

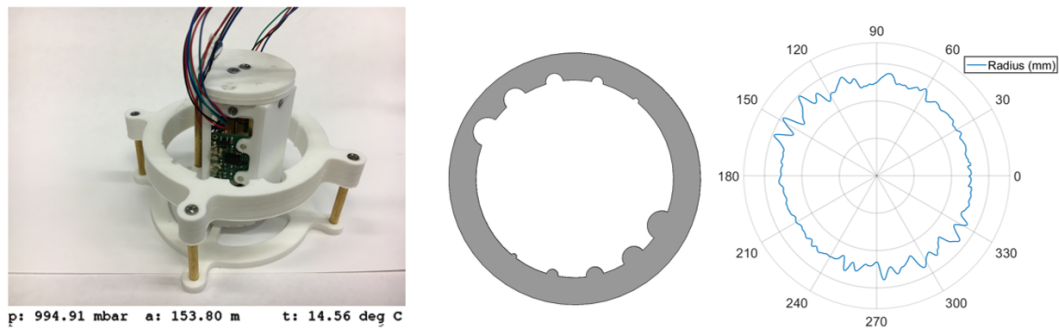


Figure 4.3: Instrumentation module testing.

Preliminary results demonstrate the potential for the detection of anomalies in tubes and pipes using the LiDAR sensor. Data from the environmental sensor is also shown and includes pressure (p), altitude (a), and temperature (t). It should be noted that the camera was not installed during this testing.

Another component of the instrumentation module tested was the slip-ring. A testbed was designed and 3-D printed for housing the disks attached to a electric motor for rotation. The power and signal tracks are fixed on the bed, while the brush block with the wires is attached to the motor shaft and rotate 360° continuously. Initially, the connection between the signal tracks and brush block were verified using a multimeter. Subsequently, the slip ring was tested while rotating with a code transmitting the data from the LiDAR sensor. The system worked well in transmitting the data from the sensor to the microcontroller without incurring electrical noise. The measurements were transmitted to a computer and recorded. The testing and data recorded can be seen on Figure 4.4.

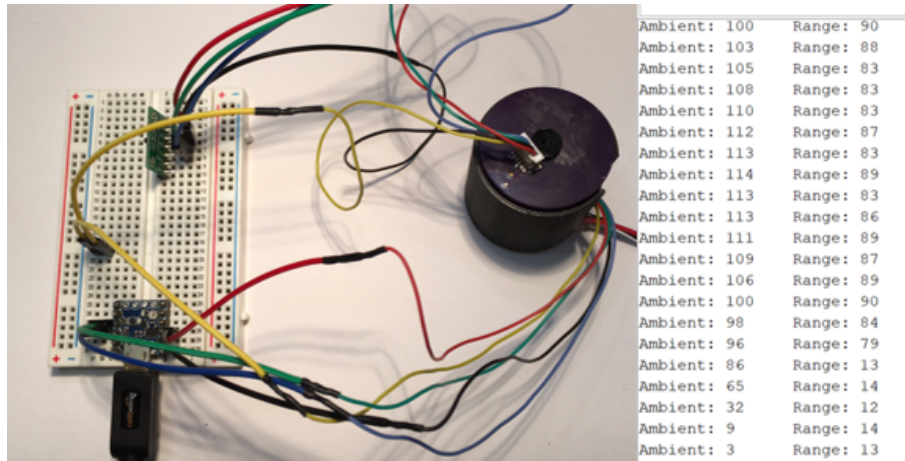


Figure 4.4: Slip ring testing.

#### 4.1.3 ULTRASONIC TRANSDUCER MODULE

The UT sensor module houses a UT sensor probe to measure tube wall thickness. The module was evaluated for its ability to obtain thickness measurements at any circumferential location within a pipe. A clear acrylic tube with a 5 cm in diameter and wall thickness of 1.6 mm was used to validate the module. The ultrasonic transducer gauge was calibrated to measure the thickness by setting the sound velocity of the probe to 2390 m/s which is specific to PVC and acrylic tubes. Since the module was not integrated with the crawler for the bench-scale testing, the stabilization mechanism was adapted to be used at both ends of the module. Figure 4.5 shows the test performed with the UT sensor module.



Figure 4.5: Measurements performed on the tube's inner surface.

Wall thickness was measured at three different locations around the inner circumference of the tube. The circumferential rotation using the spur gear set allowed the module to obtain measurements at different locations along the inner wall of the tube. As shown

in Figure 4.5, the measurements were consistent between 2.5 and 2.6 mm. The flat sensor head does not mate perfectly with the internal tube surface due its curvature. Thus, an offset must be subtracted from the measurement to obtain a more accurate reading.

To further evaluate the difference in measurements from curved surfaces tests were performed using a generic gauge. To verify the consistency of the thickness offset, a steeped steel tube section was machined to create gradually varying thicknesses along the length of the tube. The wall thickness decreased 0.198 mm at each step. Figure 4.6 shows the machined tube and the thickness steps created. Thicknesses measurements were taken from both the inside and outside surfaces of the machined tube. Since the probe had more surface contact on the outside surface, these measurements were found to represent the actual thickness. For each thickness step, twenty measurements were obtained and averaged. The results, shown in Figure 4.6, were plotted with the blue line representing the measurements from the inside surface and the red line representing the measurements from the outside surface.

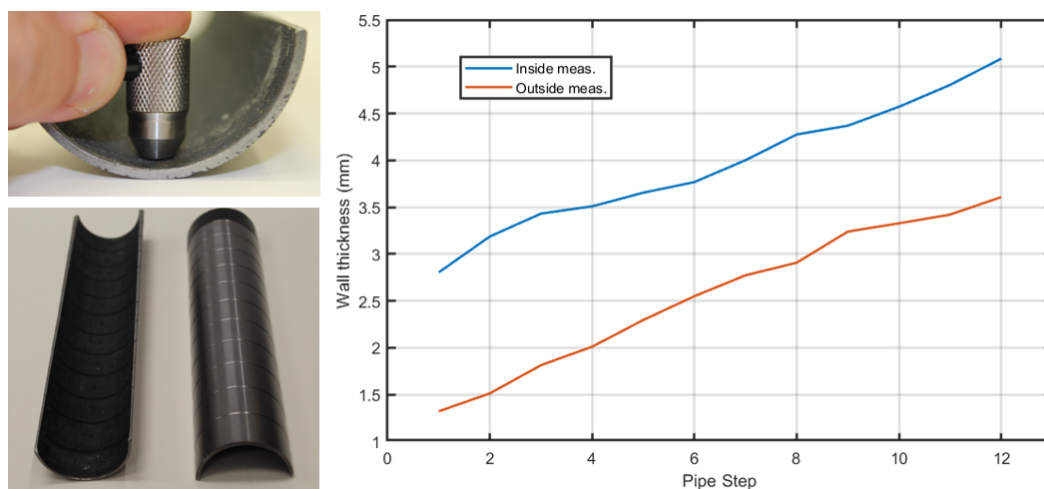


Figure 4.6: Thickness measurements obtained from the inside and outside surfaces of a tube with varying thicknesses.

Several factors can effect the accuracy of measurements using a UT sensor: the angle of incidence, the couplant, diameter of the sensor head and the curvature of the pipe. Results from this analysis show that although the measurements taken from inside

surfaces were off, the offset from the true thickness was fairly consistent and could be used to obtain reasonably accurate measurements.

#### 4.1.4 SURFACE PREPARATION MODULE

The surface preparation module was tested to evaluate its capabilities of cleaning the surface and applying the couplant gel for the UT sensor probe. Similar to the tests performed with the UT sensor module, the stabilization mechanism was adapted in both ends to maintain the module concentric within the pipe. A transparent acrylic pipe was used for better visualization of the mechanism. Figure 4.7 shows the tests performed on the surface preparation module.

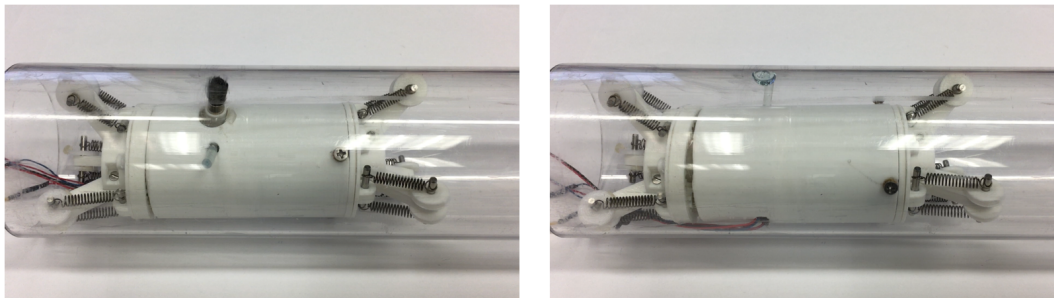


Figure 4.7: Surface preparation module.

The module was able to apply the couplant gel in different circumferential spots inside the tube. The UT sensor probe does not require a large amount of couplant. The linear actuator allowed the bush to contract and not touch the inner wall of the tube during movements, reducing drag. With regards to prepping the surface, the gear motor is limited in power but can remove small particles and deposits from the tube wall prior to taking measurements.

#### 4.2 ENGINEERING SCALE TESTING

To evaluate the crawler's performance in superheater powerplant tubes, a mockup that simulates this environment was designed and built. The mockup was constructed from acrylic plastic for visualization of the crawler when navigating. The mockup contains

eight 180° bends with 7 cm bend radii and 1.2 m straight sections connected to the bends (Figure 4.8).

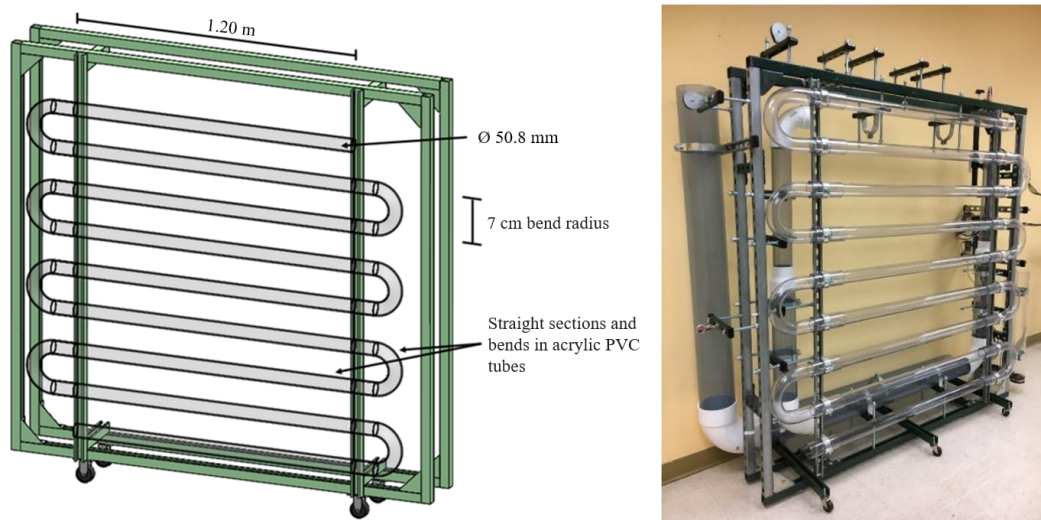


Figure 4.8: Engineering scale test mockup.

The mockup simulates the coiled structure of the boiler superheater tubes in powerplants and was designed to evaluate the tether load and wire management while the robotic crawler navigates through the bends. The straight sections are attached to the bends using plastic sleeves and can be easily disassembled if design changes are needed.

Testing was conducted to determine how the tether load changes as the crawler navigates through multiple bends and straight sections. The testing included passing a tether through the tubes and measuring the load after each 180° bend. Measurements were taken using a digital scale and repeated 7 times after each bend. Figure 4.9 shows a graph with the blue line representing the tether load averaged after each bend (x-axis on the graph).

It can be noted from Figure 4.9 that the tether load increases significantly after the fourth bend. The tether load average was 42.5 N after the 4th bend and was 132.3 N after the 5th bend. This represents an increase of 311% in tether load. Since the crawler pull force is 40 N, it is expected that the crawler can navigate through three bends before needing an additional crawler to assist in pulling the tether.

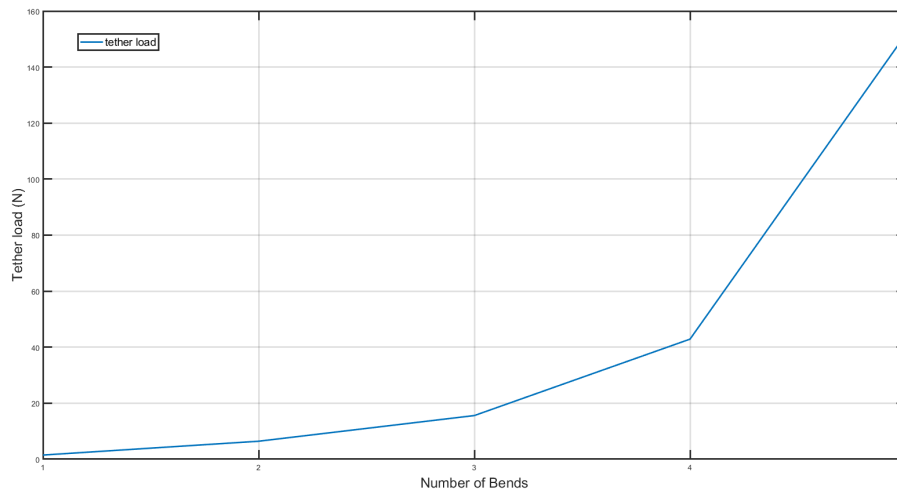


Figure 4.9: Tether load averaged.

Additional tests were performed to test the crawler’s ability to navigate through the coiled structure of the tubes. The crawler was inserted into the mockup attached to a tether providing power. Figure 4.10 shows the crawler successfully navigating through multiple straight pipe sections and bends.

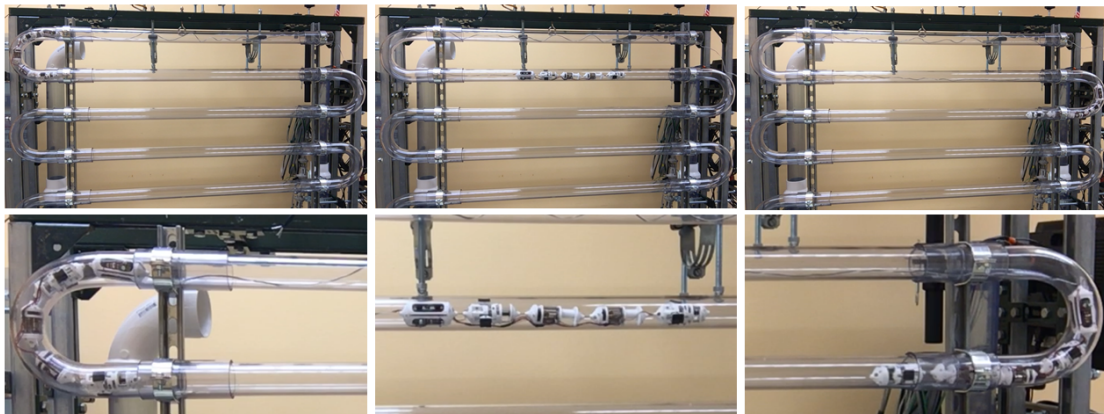


Figure 4.10: Crawler navigating the superheater tube mock-up with magnified images.

The robotic crawler successfully navigated through two bends and three straight sections in the mockup. The distance traveled was limited by the length of the tether. However, improvements can be made to increase the pull forces capabilities and reduce the tether load. For example, the motors on the extenders can use a higher reduction rate for increased torque, or different materials can cover the tether for reduced friction.

It is expected that after modifications, an additional crawler will be needed to assist in the load distribution after it has passed through 4 bends.

## 5. CONCLUSION AND RECOMMENDATIONS

The thesis described a robot that can navigate in 50.8 mm pipes containing several 180° bends. Moreover, the robotic platform can also collect data that can assess the integrity of the superheater tubes. This section provides a general assessment of the crawler and recommendations for future work.

### 5.1 RECOMMENDATIONS

The development of the robotic platform was influenced by a number of factors. This section highlights recommendations for some of these factors.

#### 5.1.1 MECHANICAL DESIGN

Almost all the components used on the robotic platform were 3-D printed. This approach allowed for fast prototyping and validation of the components designed. Although this technology can be relatively fast, 3-D printing some small components for the robot proved to be a challenge. For example, most of the gears utilized on the robot had to be re-designed or substituted for off-the-shelf components. The crawler's performance improved after using these components, demonstrating the importance of a precise connection between the parts. 3-D printing did allow for immediate evaluation of the concepts, but techniques that offer more precision such as machining should be considered for some components.

The crawler also utilized commercial off-the-shelf components that could be improved in terms of the space required. For example, the probe used in measuring wall thickness inside the UT sensor module has a length of 25 mm and was the smallest one commercially available. This component proved to be challenging to embed in the 35 mm module body. Furthermore, creating a linear actuator in the remaining space was also challenging. Due to the size constraints, another module had to be created to pre-

pare the surface for the UT sensor probe. The use of a probe specifically designed for this module could further improve the crawler's performance.

Additional improvements would come from utilizing custom designed components that are specifically aligned for this research effort. Examples include the UT sensor probe and gauge, the peristaltic pump, and the rotating brush in the instrumentation module. The use of new manufacturing methods for increased precision should also be considered. These modifications would increase the robot's reliability and improve its capabilities.

### 5.1.2 ELECTRONICS

The crawler's electronics control the module's electric motors and actuators. They were developed using commercially available components for ease of manufacturing and testing but at the loss of space efficiency. The microcontrollers, motor controllers, and current sensors utilized can be reduced in size when its components such as microchips, resistors, and capacitors are integrated into a single PCB. Thus, this board can potentially have the same functionality with a reduced size.

The creation of a PCB for the modules could also aid in creating a more efficient microcontroller for the crawler. The PICO microcontroller was used in the majority of the PCBs developed, due to size constraints. This microcontroller is one of the most versatile on the market, due to its size and reliability. However, it does not deliver enough current to power all the electronics utilized and has a limited number of analog and digital pins.

The development of PCBs with embedded microchips would improve the robotic platform capabilities and save space. In addition, the integration of the microchips into a PCB would create more space for the mechanical components of the crawler and potentially reduce the total amount of modules. That would be possible by integrating the electronics of each module of the peristaltic crawler into the free space inside their front caps, eliminating the necessity of the electronics module.

### 5.1.3 COMMUNICATION PROTOCOL

The CAN-Bus communication was tested and integrated into all modules and proved its efficiency in sending and receiving data. In addition, the protocol has very little latency and provides a simple means to integrate new modules into the communication line. However, this communication protocol requires the integration of another electronic board into each module. Another drawback of the CAN-Bus communication is the limited data size, which can transmit and receive only 14 bytes on each cycle. From the total amount of bytes transmitted by the CAN-Bus, 6 of them are already reserved for the communication mask and filter, providing only 8 bytes open to the users communication.

This protocol was used due to its performance in sending and receiving data for long lines distance. It is a reliable communication protocol that can be further improved. The microchips necessary for the CAN-Bus communication can be integrated into a single PCB, eliminating another electronic board's necessity. Research is needed to verify if this communication protocol can afford higher data processing to increase the data size transmitted on each pulse.

## 5.2 CONCLUSION AND FUTURE WORK

This thesis describes a robotic crawler that was developed and can navigate through 5 cm diameter tubes similar to those found in fossil energy power plants. The base modules for navigation include two grippers and two extenders. The maximum pull force of the system is limited by the strength of the extenders which is 40 N. Once the drag force of the tether reaches this value, an additional crawler is needed to assist in the load distribution. Testing of the crawler system demonstrated its ability to navigate through multiple straight sections and 180° bends.

Additional modules have been developed that include an electronics module, a UT sensor module, a surface preparation module, and an instrumentation module. Initial

testing of the modules demonstrate the system's ability to inspect the integrity and conditions within 5 cm diameter tubes.

Although the peristaltic crawler was developed for application in the superheater tubes found in fossil energy powerplants, it can be used in different environments. The robot is modular and can navigate through sharp bends and straight sections contained in 50.8 mm diameter piping. For example, alternative industries that the robot can be applied in are nuclear, gas and oil, as these industries also use small diameter piping in certain systems. By making simple modifications to the inspection modules and sensors, the robot can be specialized towards whichever industry it is being considered for.

The modular crawlers developed will be integrated with a common tether to form the proposed inspection tool. This tool is composed of several modular units, carrying embedded sensory, tethered to a control box for the user interface. A conceptual drawing is shown in Figure 5.1.

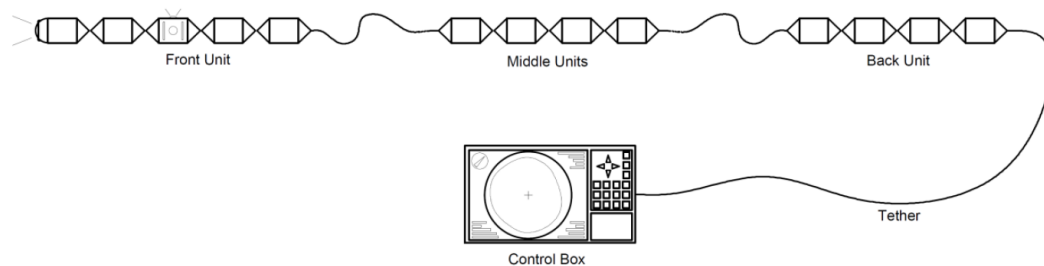


Figure 5.1: Integrated crawler system (inspection tool) concept.

## BIBLIOGRAPHY

- [1] 8.5 Curved Surface Correction (CSC) | Olympus IMS. URL: <https://www.olympus-ims.com/en/ndt-tutorials/flaw-detection/csc/> (visited on 08/29/2021).
- [2] Geogy J. Abraham, Vivekanand Kain, and Niraj Kumar. “Cracking of superheater tube in a captive power plant”. In: *Corrosion Engineering Science and Technology* 53 (2018), pp. 98–104. ISSN: 17432782. DOI: 10.1080/1478422X.2017.1386018.
- [3] *Accurate and Informative Data: The LiDAR Advantage - RedZone Robotics*. URL: <https://redzone.com/nr/the-lidar-advantage/> (visited on 09/28/2021).
- [4] Md Hazrat Ali et al. “Development of a robot for boiler tube inspection”. In: *ICINCO 2018 - Proceedings of the 15th International Conference on Informatics in Control, Automation and Robotics 2*. Icinco (2018), pp. 534–541. DOI: 10.5220/0006930205340541.
- [5] Mohamed G. Alkalla, Mohamed A. Fanni, and Abdelfatah M. Mohamed. “A novel propeller-type climbing robot for vessels inspection”. In: *IEEE/ASME International Conference on Advanced Intelligent Mechatronics, AIM 2015-Augus*. July (2015), pp. 1623–1628. DOI: 10.1109/AIM.2015.7222776.
- [6] D N Badodkar et al. “EMAT Integrated with Vertical Climbing Robot for Boiler Tube Inspection”. In: *Proceedings of the National Seminar Exhibition on Non-Destructive Evaluation (2009)*, pp. 32–36. URL: <https://www.ndt.net/article/nde-india2009/index.htm>.
- [7] William Alexander Blyth. “Robotic Pipe Inspection : System Design , Locomotion and Control”. PhD thesis. Imperial College London, 2017, p. 234.
- [8] Alexander S. Boxerbaum et al. “Continuous wave peristaltic motion in a robot”. In: *International Journal of Robotics Research* 31.3 (2012), pp. 302–318. ISSN: 02783649. DOI: 10.1177/0278364911432486.
- [9] C. H. Chen, ed. *Ultrasonic and Advanced Methods for Nondestructive testing and Material Characterization*. Vol. 148. Singapore: World Scientific Publishing Co., 2007, pp. 148–162. ISBN: 9789812704092.
- [10] Roland T Chin and A N I Charles A Harlow. “Automated Visual Inspection : A Survey”. In: *IEEE Transactions on Pattern Analysis and Machine Intelligence* 4.6 (1982), pp. 557–573.
- [11] Changhwan Choi, Seungho Jung, and Seungho Kim. “Feeder pipe inspection robot with an inch-worm mechanism using pneumatic actuators”. In: *International Journal of Control, Automation and Systems* 4.1 (2006), pp. 87–95. ISSN: 15986446.
- [12] B. B.V.L. Deepak, M. V.A.Raju Bahubalendruni, and B. B. Biswal. “Development of in-pipe robots for inspection and cleaning tasks: Survey, classification and comparison”. In: *International Journal of Intelligent Unmanned Systems* 4.3 (2016), pp. 182–210. ISSN: 20496435. DOI: 10.1108/IJIUS-07-2016-0004.

- [13] F. Dehnavi, A. Eslami, and F. Ashrafizadeh. “A case study on failure of superheater tubes in an industrial power plant”. In: *Engineering Failure Analysis* 80. June (2017), pp. 368–377. ISSN: 13506307. DOI: 10.1016/j.engfailanal.2017.07.007.
- [14] Edwin Dertien et al. “Design of a robot for in-pipe inspection using omnidirectional wheels and active stabilization”. In: *Proceedings - IEEE International Conference on Robotics and Automation* March 2016 (2014), pp. 5121–5126. ISSN: 10504729. DOI: 10.1109/ICRA.2014.6907610.
- [15] R. Dhayalan and Krishnan Balasubramaniam. “A hybrid finite element model for simulation of electromagnetic acoustic transducer (EMAT) based plate waves”. In: *NDT and E International* 43.6 (2010), pp. 519–526. ISSN: 09638695. DOI: 10.1016/j.ndteint.2010.05.008.
- [16] Markus Eich and Thomas Vögele. “Design and control of a lightweight magnetic climbing robot for vessel inspection”. In: *2011 19th Mediterranean Conference on Control and Automation, MED 2011* (2011), pp. 1200–1205. DOI: 10.1109/MED.2011.5983075.
- [17] *EMAT Technology*. URL: <https://www.innerspec.com/emat-technology> (visited on 08/29/2021).
- [18] W. Fischer et al. “Very compact climbing robot rolling on magnetic hexagonal cam-discs, with high mobility on obstacles but minimal mechanical complexity”. In: *Joint 41st International Symposium on Robotics and 6th German Conference on Robotics 2010, ISR/ROBOTIK 2010 2* (2010), pp. 1239–1245.
- [19] Atul A. Gargade and Dr. Shantipal S. Ohol. “Development of In-pipe Inspection Robot”. In: *IOSR Journal of Mechanical and Civil Engineering* 13.04 (2016), pp. 64–72. ISSN: 2320334X. DOI: 10.9790/1684-1304076472.
- [20] Lianwu Guan et al. “A comprehensive review of micro-inertial measurement unit based intelligent PIG multi-sensor fusion technologies for small-diameter pipeline surveying”. In: *Micromachines* 11.9 (2020). ISSN: 2072666X. DOI: 10.3390/MI11090840.
- [21] James J Heckman, Rodrigo Pinto, and Peter A. Savelyev. *Heat recovery steam generator technology*. Ed. by Convey Maria. United Kingdom: WP Woodhead Publishing, 1967, p. 411. ISBN: 978-0-08-101940-5.
- [22] *High Thermal Efficiency Steam Boiler Superheater for Power Plant Boiler*. URL: <https://www.coowor.com/p/20170802131759693HGN66Y/High-Thermal-Efficiency-Steam-Boiler-Superheater-for-Power-Plant-Boiler.htm> (visited on 08/29/2021).
- [23] *HydroFORM/RexoFORM | Olympus IMS*. URL: <https://www.olympus-ims.com/pt/corrosion-solutions/hydroform-rexoform/> (visited on 09/06/2021).
- [24] Faisal I. Khan and Mahmoud M. Haddara. “Risk-based maintenance (RBM): A quantitative approach for maintenance/inspection scheduling and planning”. In: *Journal of Loss Prevention in the Process Industries* 16.6 (2003), pp. 561–573. ISSN: 09504230. DOI: 10.1016/j.jlp.2003.08.011.

- [25] Yun Jong Kim, Kyung Hyun Yoon, and Young Woo Park. “Development of the inpipe robot for various sizes”. In: *IEEE/ASME International Conference on Advanced Intelligent Mechatronics, AIM 764* (2009), pp. 1745–1749. DOI: 10.1109/AIM.2009.5229808.
- [26] Young-sik Kwon and Byung-ju Yi. “Design and Motion Planning of a Two-Module”. In: *IEEE Transactions on Robotics* 28.3 (2012), pp. 681–696. ISSN: 15523098.
- [27] Domenico Longo and Giovanni Muscato. “A modular approach for the design of the Alicia3 climbing robot for industrial inspection”. In: *Industrial Robot* 31.2 (2004), pp. 148–158. ISSN: 0143991X. DOI: 10.1108/01439910410522838.
- [28] Bruce G Miller. *Clean Coal Engineering Technology*. Burlington: Butterworth-Heinemann, 2011. ISBN: 978-1-85617-710-8. URL: <http://www.sciencedirect.com/science/book/9781856177108>.
- [29] George H. Mills, Andrew E. Jackson, and Robert C. Richardson. “Advances in the inspection of unpiggable pipelines”. In: *Robotics* 6.4 (2017). ISSN: 22186581. DOI: 10.3390/robotics6040036.
- [30] Junghu Min et al. “Development and controller design of wheeled-type pipe inspection robot”. In: *Proceedings of the 2014 International Conference on Advances in Computing, Communications and Informatics, ICACCI 2014* (2014), pp. 789–795. DOI: 10.1109/ICACCI.2014.6968543.
- [31] Paul E. Mix. *Introduction to Nondestructive Testiong*. 2nd ed. Hoboken, 2005, p. 620. ISBN: 13 978-0-471-42029-3.
- [32] A. Nishi and H. Miyagi. “Propeller Type Wall-Climbing Robot for Inspection Use”. In: *Automation and robotics in construction X: proceedings of the 10th International Symposium on Automation and Robotics in Construction (ISARC)* (2017), pp. 189–196. DOI: 10.22260/isarc1993/0025.
- [33] Harutoshi Ogai and Bishakh Bhattacharya. *Pipe Inspection Robots for Gas and Oil Pipelines*. Vol. 89. 2018, pp. 13–43. ISBN: 9788132237518. DOI: 10.1007/978-81-322-3751-8\_2.
- [34] Harutoshi. Ogai and Bishakh. Bhattacharya. *Pipe inspection robots for structural health and condition monitoring*. Springer, 2018, p. 213. ISBN: 978-81-322-3749-5.
- [35] Manabu Ono and Shigeo Kato. “A study of an earthworm type inspection robot movable in long pipes”. In: *International Journal of Advanced Robotic Systems* 7.1 (2010), pp. 85–90. ISSN: 17298814. DOI: 10.5772/7248.
- [36] P. A. Petcher, M. D.G. Potter, and S. Dixon. “A new electromagnetic acoustic transducer (EMAT) design for operation on rail”. In: *NDT and E International* 65 (2014), pp. 1–7. ISSN: 09638695. DOI: 10.1016/j.ndteint.2014.03.007. URL: <http://dx.doi.org/10.1016/j.ndteint.2014.03.007>.
- [37] *Powder Coating Thickness Measurement - Steel, Aluminum, Wood | Resources | DeFelsko*. URL: <https://www.defelsko.com/resources/powder-coating-thickness-measurement> (visited on 08/29/2021).
- [38] Ravi Prakash. *Non-Destructive Testing Techniques*. Kent: New Academic Science limited, 2012, p. 145. ISBN: 978 1 906574 42 0.

- [39] Jinwei Qiao, Jianzhong Shang, and Andrew Goldenberg. “Development of inch-worm in-pipe robot based on self-locking mechanism”. In: *IEEE/ASME Transactions on Mechatronics* 18.2 (2013), pp. 799–806. ISSN: 10834435. DOI: 10.1109/TMECH.2012.2184294.
- [40] Rayaprolu Kumar. *Boilers for Power and Process*. 1st Editio. Boca Raton: CRC Press, 2009, p. 811. ISBN: 9781420075373.
- [41] Hyouk Ryeol and Se-gon Roh. “In-pipe Robot with Active Steering Capability for Moving Inside of Pipelines”. In: *Bioinspiration and Robotics Walking and Climbing Robots* 2014 (2007). DOI: 10.5772/5512.
- [42] Patrick Schoeneich et al. “TRIPILLAR: A miniature magnetic caterpillar climbing robot with plane transition ability”. In: *Robotica*. Vol. 29. 7. 2011, pp. 1075–1081. DOI: 10.1017/S0263574711000257.
- [43] Ramesh K. Shah and Duan P. Sekuli. *Fundamentals of Heat Exchanger Design*. Hoboken: John Wiley Sons, Inc., 2003, pp. 673–734. ISBN: 0-471-32171-0. DOI: 10.1002/9780470172605.ch10.
- [44] Jason R Soto. “Design of a Robotic Inspection Platform for Structural Health Monitoring”. PhD thesis. Florida International University, 2020.
- [45] Mahmoud Tavakoli et al. “OmniClimbers: Omni-directional magnetic wheeled climbing robots for inspection of ferromagnetic structures”. In: *Robotics and Autonomous Systems* 61.9 (2013), pp. 997–1007. ISSN: 09218890. DOI: 10.1016/j.robot.2013.05.005. URL: <http://dx.doi.org/10.1016/j.robot.2013.05.005>.
- [46] *U.S. Energy Information Administration (EIA)*. URL: <https://www.eia.gov/tools/faqs/faq.php?id=427&t=3> (visited on 08/29/2021).
- [47] Hee-Joo Yeo. “Development of a Robot System for Repairing a Underground Pipe”. In: *Journal of the Korea Academia-Industrial cooperation Society* 13.3 (2012), pp. 1270–1274. ISSN: 1975-4701. DOI: 10.5762/kais.2012.13.3.1270.
- [48] Basem F Yousef and Nabil Bastaki. “Worm Robot with Dynamic Adaptation to Pipe Diameter for In - Pipe Inspection”. In: 3.10 (2014), pp. 286–292.
- [49] Xiao Yu et al. “Development of a novel in-pipe walking robot”. In: *2015 IEEE International Conference on Information and Automation, ICIA 2015 - In conjunction with 2015 IEEE International Conference on Automation and Logistics August* (2015), pp. 364–368. DOI: 10.1109/ICInfA.2015.7279314.